

Kelvin Helmholtz Instability in Dusty Plasma with Kappa Distributed Species



By

Jabir Khan

(367-FBAS/MSPHY/F15)

Supervisor

Dr. Mushtaq Ahmad

Professor

Department of Physics, FBAS,

IIU, Islamabad

**Department of Physics
Faculty of Basic and Applied Sciences
International Islamic University, Islamabad**

(2017)





Accession No TH:18071

MS
530-44
JAK

Dusty plasmas
Kappa distribution

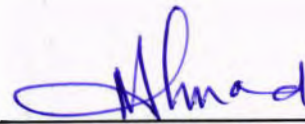
Kelvin Helmholtz Instability in Dusty Plasma with Kappa Distributed Species

By

Jabir Khan

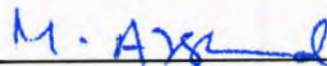
(367-FBAS/MSPHY/F15)

This Thesis submitted to Department of Physics International Islamic University,
Islamabad for the award of degree of MS Physics.



CHAIRMAN
DEPT. OF PHYSICS
International Islamic University
Islamabad

Chairman Department of Physics
International Islamic University Islamabad.



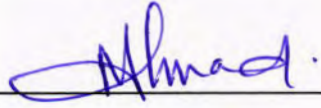
Dean Faculty of Basic and Applied Sciences
International Islamic University Islamabad.

Final Approval

It is certified that the work presented in this thesis entitled “**Kelvin Helmholtz Instability in Dusty Plasma with Kappa Distributed Species**” by **Jabir Khan**, registration No.367-FBAS/MSPHY/F15 fulfills the requirement for the award of degree of MS Physics from Department of Physics, International Islamic University, Islamabad, Pakistan.

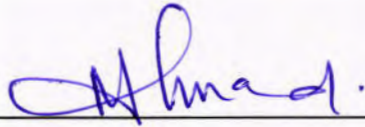
Viva Voce Committee

Chairman

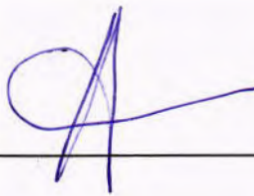


(Department of Physics)

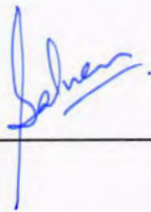
Supervisor



External Examiner



Internal Examiner

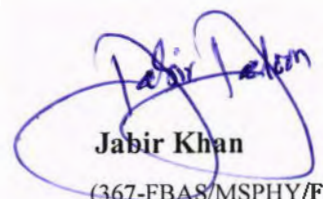


بِسْمِ اللَّهِ الرَّحْمَنِ الرَّحِيمِ

**DEDICATED
TO
MY BELOVED PARENTS
AND
RESPECTED TEACHERS**

Declaration of Originality

I, **Jabir Khan** Reg. No. 367-FBAS/MSPHY/F15 student of MS Physics (Session 2015-2017), hereby declare that the work presented in the thesis titled “**Kelvin Helmholtz Instability in Dusty Plasma with Kappa Distributed Species**” in partial fulfillment of MS degree in Physics from International Islamic University Islamabad, Pakistan, is my own work and has not been published or submitted as research work or thesis in any form in any other university or institute in Pakistan or abroad.

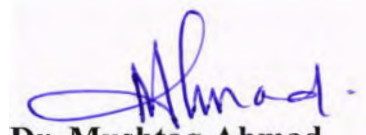


Jabir Khan
(367-FBAS/MSPHY/F15)

Dated: _____

Forwarding Sheet by Research Supervisor

The thesis titled “**Kelvin Helmholtz Instability in Dusty Plasma with Kappa Distributed Species**” submitted by **Jabir Khan** (Reg. No. 367-FBAS/MSPHY/F15) in partial fulfillment of MS degree in Physics has been completed under my guidance and supervision. I am satisfied with the quality of his research work and allow him to submit this thesis for further process to graduate with Master of Science degree from Department of Physics, as per International Islamic University Islamabad, Pakistan, rules and regulations.



Dr. Mushtaq Ahmad
Professor
Department of Physics,
International Islamic University,
Islamabad.

Dated: _____

Acknowledgment

All glory be to ALLAH, the unfailing fountain and containing source of knowledge, who conferred upon us both the ability to contribute to the eternally, flowing ocean of knowledge, a few drops which in its turn helps man in his, universe and ultimately ALLAH recognition; indeed, our drops can easily be picked out an account of them unique color, flavor and worth. The role model life of the holy prophet (PBUH) has remained a beacon house in spurring the successful accomplish meant of this glorious task.

This work would have not been possible without the committed contribution of many individuals. I wish to thanks my MS supervisor, **Prof. Dr. Mushtaq Ahmad**, for all of his support, advice and guidance during the research work. He was always there to listen and to give advice. He showed me different ways to approach a research problem and the need to be persistent to accomplish any goal. Without his encouragement and constant guidance, I could not have completed my work. My heartiest thanks are to all members of the Theoretical Plasma Physics Group at the Department of Physics, International Islamic University Islamabad, notably to **Muhammad Farooq, Qasim Jan, and Sibghatullah Khan Marwat**.

Last but never least; I would like to mention my sweat **mother**, respected **father**, brother's (**Shahid Jadoon, Tahir Jadoon and Imad Jadoon**) **sisters and sister in-law** for their love, and care towards me. Their prayers always give me strength and courage to move ahead.

Jabir Khan
(367-FBAS/MSPHY/F-15)

Contents

1	Introduction and Literature survey	8
1.1	Plasma Physics	8
1.2	Multi-component plasma	10
1.3	Dusty Plasma	10
1.3.1	Macroscopic Neutrality	11
1.3.2	Debye Shielding	11
1.3.3	Characteristics Frequency	12
1.3.4	Coulomb Coupling Parameter	12
1.3.5	Charging Mechanisms	12
1.4	Occurrence of dusty plasma	13
1.4.1	Interplanetary space	14
1.4.2	Planetary rings system	15
1.4.3	Earth's atmosphere	15
1.5	Applications of dusty plasma	16
1.6	Maxwellian and non-Maxwellian distribution functions	18
1.6.1	Maxwellian Distribution Function	18
1.6.2	Non Maxwellian Distribution Functions	19
1.7	Kappa Distribution	24
1.8	Waves and Instabilities in Dusty Plasma	26
1.8.1	Waves in dusty plasma	26
1.8.2	Instabilities in Dusty Plasma	28
1.9	Kelvin Helmholtz Instability	30
1.10	Layout of Thesis	32

2 Kelvin Helmholtz Instability in Dusty Plasma with Kappa Distributed Species	34
2.1 Introduction	34
2.2 Basic Formulation	36
2.3 Results and discussions	44
2.3.1 KH- instability with positive dust polarity	45
2.3.2 KH-instability analysis with negative dust polarity	53
3 Summary and Conclusions	62
Bibliography	63

List of Figures

1.1	MHD generator [3].	9
1.2	Treatment of a patient with the help of plasma based device [7].	9
1.3	An image of inter-planetary dust [24].	14
1.4	An image of Saturn's rings, taken by spacecraft [29].	16
1.5	A view of Notilucent clouds after sunset [33].	17
1.6	Figure of an photovoltaic source of electric energy, in which dust particles are used [44].	18
1.7	The Maxwellian velocity distribution [45].	19
1.8	The Cairn's distribution function for different values of α [53]	21
1.9	A graphical representation of (r, q) for different values of index q and r [63].	23
1.10	Kappa (<i>VDFs</i>) for different value of κ [72].	25
1.11	A schematic diagraph of most common formulations of the kappa distribution for direct use in space plasma analyses [80].	26
1.12	An image of a DAWs pattern taken by video camera [87].	27
1.13	An image of <i>RT instability, where heavy fluid is supported by lighter fluid</i> [96].	30
1.14	Configuration for the <i>Kelvin – Helmholtz</i> instability [105].	32
2.1	The graphical representation of normalized frequency ω_{r1} of KH modes. (a) as a function of K_y for different values of $\kappa = 2$ (red dotted line), $\kappa = 3$ (blue dotted line) and $\kappa = 4$ (green dotted line), while (b) is the 3-dimensional view with k_y and κ . All others parameters are taken arbitrary from section of result and discussion.	46

2.2	The graphical representation of growth rate Γ_1 of KH modes. (a) as a function of k_y for different values of $\kappa = 2$ (red dotted line), $\kappa = 3$ (blue dotted line) and $\kappa = 4$ (green dotted line) and (b) is the 3-dimensional view with K_y and κ	47
2.3	(a) Variation of real frequency ω_{r1} as a function of k_y , for different values of electron temperature such that $T_e = 1.15 \times 10^4$ (red dotted) line and for $T_e = 1.15 \times 10^6$ (blue dotted line), while (b) is the 3-D representation of frequency with effect of temperature of electron.	48
2.4	(a) Variation of real frequency Γ_1 as a function of k_y , for different values of electron temperature such that $T_e = 1.15 \times 10^4$ (red dotted) line and for $T_e = 1.15 \times 10^6$ (blue dotted line), while (b) is the 3-D representation of frequency with effect of temperature of electron.	49
2.5	(a) Variation of real frequency ω_{r1} as a function of wave vector k_y , for different values of magnetic field such that $B = 0.0004$ (red dotted line), $B = 0.0005$ (blue dotted line) and $B = 0.0006$ (black dotted line), while (b) is the 3-D representation of frequency with effect of magnetic field. The physical parameters are taken from the section of result and discussions.	50
2.6	(a) Variation of growth rate Γ_1 as a function of wave vector k_y , for different values of magnetic field such that $B = 0.0004$ (red dotted line), $B = 0.0005$ (blue dotted line) and $B = 0.0006$ (black dotted line), while (b) is the 3-D representation of growth rate with effect of magnetic field.	51
2.7	(a) Variation of real frequency ω_{r1} as a function of wave vector k_y , for different values of sheared flow such that $A = 0.01$ (red dotted line), $A = 0.02$ (blue dotted line) and $A = 0.03$ (black dotted line), while (b) is the 3-D representation of frequency with effect of sheared flow. . . .	52

2.8	(a) Variation of growth rate Γ_1 as a function of wave vector K_y , for different values of sheared flow such that $A = 0.01$ (red dotted line), $A = 0.02$ (blue dotted line) and $A = 0.03$ (black dotted line), while (b) is the 3-D representation of growth rate with effect of sheared flow. . .	53
2.9	The graphical representation of normalized frequency ω_{r1} of KH modes. (a) as a function of k_y for different values of $\kappa = 2$ (red dotted line), $\kappa = 3$ (blue dotted line) and $\kappa = 4$ (green dotted line), while (b) is the 3-dimensional view with k_y and κ	54
2.10	The graphical representation of normalized frequency ω_{r1} of KH modes. (a) as a function of k_y for different values of $\kappa = 2$ (red dotted line), $\kappa = 3$ (blue dotted line) and $\kappa = 4$ (green dotted line), while (b) is the 3-dimensional view with K_y and κ	55
2.11	(a) Variation of real frequency ω_{r1} as a function of k_y , for different values of electron temperature such that $T_e = 1.15 \times 10^4$ (red dotted) line and for $T_e = 1.15 \times 10^6$ (blue dotted line), while (b) is the 3-D representation of frequency with effect of temperature of electron.	56
2.12	(a) Variation of real frequency Γ_1 as a function of k_y , for different values of electron temperature such that $T_e = 1.15 \times 10^4$ (red dotted) line and for $T_e = 1.15 \times 10^6$ (blue dotted line), while (b) is the 3-D representation of frequency with effect of temperature of electron.	57
2.13	(a) Variation of real frequency ω_{r1} as a function of wave vector k_y , for different values of magnetic field such that $B = 0.0004$ (red dotted line), $B = 0.0005$ (blue dotted line) and $B = 0.0006$ (black dotted line), while (b) is the 3-D representation of frequency with effect of magnetic field. The physical parameters are taken from the section of result and discussion.	58

- 2.14 (a) Variation of growth rate Γ_1 as a function of wave vector K_y , for different values of magnetic field such that $B = 0.0004$ (red dotted line), $B = 0.0005$ (blue dotted line) and $B = 0.0006$ (black dotted line), while (b) is the 3-D representation of growth rate with effect of magnetic field. 59
- 2.15 (a) Variation of real frequency ω_{r1} as a function of wave vector k_y , for different values of sheared flow such that $A = 0.01$ (red dotted line), $A = 0.02$ (blue dotted line) and $A = 0.03$ (black dotted line), while (b) is the 3-D representation of frequency with effect of sheared flow. . . . 60
- 2.16 (a) Variation of growth rate Γ_1 as a function of wave vector k_y , for different values of sheared flow such that $A = 0.01$ (red dotted line), $A = 0.02$ (blue dotted line) and $A = 0.03$ (black dotted line), while (b) is the 3-D representation of growth rate with effect of sheared flow. . . . 61

Abstract

The different modes of Kelvin Helmholtz instability are studied in dusty plasma with Kappa distributed electrons, while dust and ions are consider Maxwellian. The K-H instability arises in dusty plasma due to dust sheared or relative velocity between two layers of dust. In four component dusty plasma the polarity effect is investigated. Instability analysis is also perform. By changing the value of different parameters such as electron temperature, magnetic field, kappa index κ , and sheared flow we study the growth rate and frequency of K-H modes. Instability relation and condition are derived for both positive and negative polarity of the dust. All the parameters mentioned above cause effect on growth rate and frequency of K-H modes. Relevance of the work with respect to / planetary rings dusty plasma is pointed out.

Chapter 1

Introduction and Literature survey

1.1 Plasma Physics

The plasma is a Greek word $\pi\lambda\alpha\sigma\mu\alpha$ means something prepared, appropriated by Tonks and Langmuir in 1929. It is used to describe the general diversity of macroscopically impartial constituents comprising numerous cooperating electrons and ionized atoms which display common performance. The beauty of these charge constituents is that they have equal charge densities in which charge particle interactions are collective rather than binary [1]. Plasma often called fourth state of matter and it is believed that 99% of visible universe consists of plasma state. The man-made plasma is the fusion reaction, gas discharge, arc welder, arc inside fluorescent lamp and electric arc etc. The global plasma examples are ionosphere, lightning and flames (i.e. fire etc.). The astrophysical plasma is found in stellar interior, gaseous nebula etc. Our sun is also a plasma state. Near earth region it is found in magnetosphere, Van Allen belts and solar wind puffing from the sun [2].

Plasma have vast applications in every field of life. For the generation of power, plasma is used in fusion reactions. This is also a source of energy of sun and stars. In the magnetohydrodynamics (MHD) generators, the kinetic energy of plasma is converted into electrical energy. While its reverse process is jet propulsion. Gas discharge is an example of thermionic energy convertor. Similarly, mercury rectifiers, sparks gaps and ignitors used for plasma jets. The space vehicles are also communicated through space

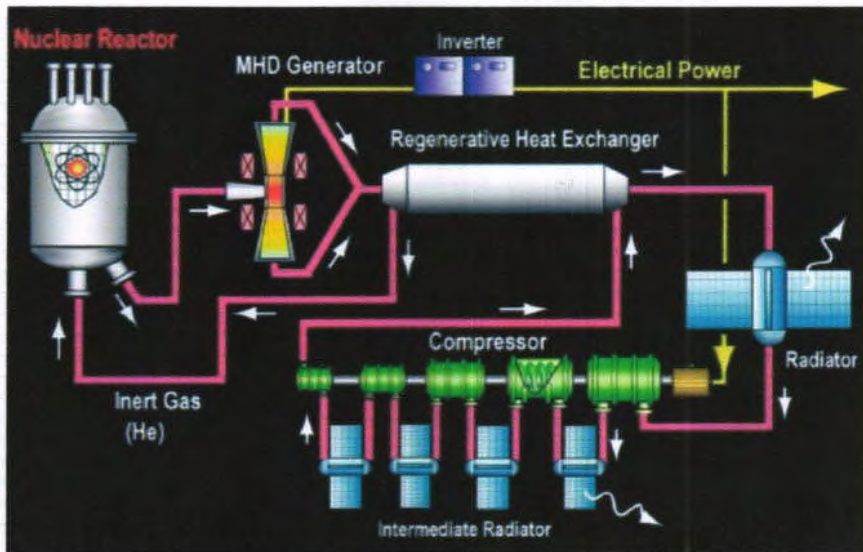


Figure 1.1: MHD generator [3].

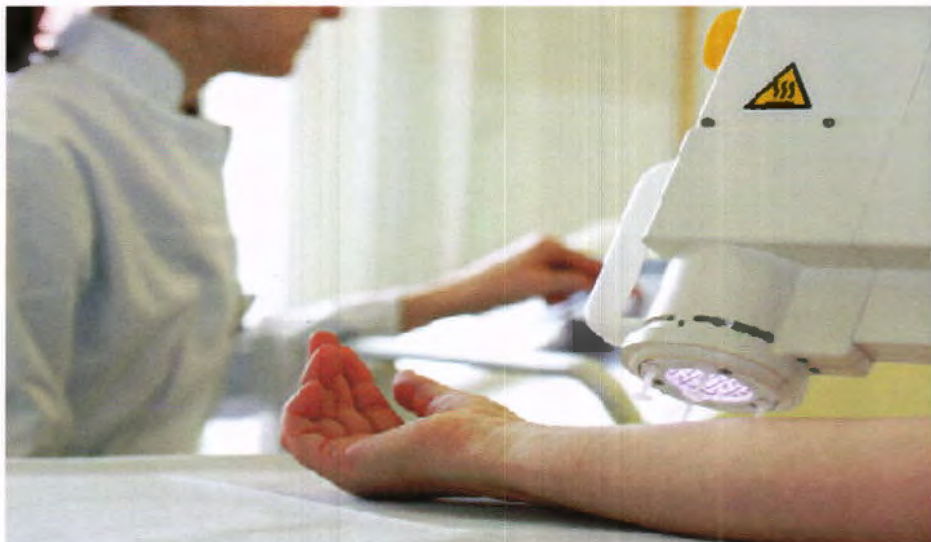


Figure 1.2: Treatment of a patient with the help of plasma based device [7].

plasma [4]. The MHD generator is shown in Fig. 1.1.

Keeping in view plasma miracles the plasma medicine has settled into a pioneering field of research from last few years showing high potential for manufacturing of medicines and sterilizing of medical devices [5]. The cold plasma is used for dealing of fungal infections, tissues, dermatology and blood coagulation etc. Similarly, hot plasma is used for tumor treatment from last 30 years [6]. A plasma based device as shown in Fig. 1.2.

1.2 Multi-component plasma

Generally, plasma contains electrons and ions. The presence of extra species besides electrons and ions known as multi-component plasma. These extra species may be positron, negative ions or dust, termed as electron positron ion plasma, multi ions or pair ion plasma and dusty plasma respectively. The plasma consist of negative ions exists in astrophysical environment and can be produced in laboratories by several methods. The occurrence of pair ion plasma and its significance have been studied experimentally [8] and theoretically [9]. Similarly, electron–positron–ion plasmas is also investigated in astrophysical plasma atmosphere such as magnetosphere[10], solar winds[11] and in the nucleus of many galaxies[12], and can be produced in laboratory for the study of different modes of plasma.

1.3 Dusty Plasma

We are familiar that dust is a common thing can be found every where in universe and cause disturbances in our life. The presence of dust particles in plasma called dusty plasma. . The size of these dust particles ranges from few nanometers to several hundred of microns, and massive than electrons and ions. Generally, these particles are solids but they can be liquids droplets or fluffy ice crystals, or dielectrics e.g. SiO_2 or conducting materials having shapes like rods or spheres or pancakes [13]. These dust particles acquired charge either positive or negative [14], when inter into plasma system. A lot of theoretical and experimental work on the occurrence of really massive and highly charged static dust grains have shown that they introduce new physical mechanism and modification of the present plasma wave spectra along with different eigen modes. The dust in plasma and dusty plasma are two interesting and different things. The condition $r_d \ll \lambda_D < a$ implies dust is present in plasma and get charge by interaction and cause little influence on plasma. While the condition $r_d \ll a < \lambda_D$ means many particles in Debye sphere, and reverse otherwise. Here r_d , and λ_D are the radius, and Debye length of dust particulates respectively and a is the distance of intergrains [15]. For the proper understanding of dusty plasma, we discuss its basic

characteristics.

1.3.1 Macroscopic Neutrality

Except external perturbations, it is observed that at macroscopic level dusty plasma is neutral and total charge in it is zero. The neutrality condition for dusty plasma is

$$Z_i en_{i0} = en_{e0} - Z_d en_{d0} \quad (1.1)$$

Here e is elementary charge $q_i = Z_i e$ with $Z_i = 1$ is charge of ion and $q_{d\pm} = \pm Z_{d\pm} e$ is charge of dust species. Z_d are the number of charges which are present on the surface of dust species.

1.3.2 Debye Shielding

It is dynamic beauty of a dusty plasma to shield the electric field of an individual or surface with non-zero potential. It is defined as the distance over which the effect of electric field of specific charged particle is felt by other charged particles inside the plasma. The dusty plasma Debye radius is given as

$$\lambda_D = \frac{\lambda_{De} \lambda_{Di}}{\sqrt{\lambda_{De}^2 + \lambda_{Di}^2}} \quad (1.2)$$

Here

$$\lambda_{De} = \left(\frac{K_B T_e}{4\pi n_{e0} e^2} \right)^{\frac{1}{2}} \quad (1.3)$$

and

$$\lambda_{Di} = \left(\frac{K_B T_i}{4\pi n_{i0} e^2} \right)^{\frac{1}{2}} \quad (1.4)$$

are the electron and ion Debye radii respectively. Here are two possibilities if thickness of sheet is determined by temperature and number density of ions then $n_{e0} \ll n_{i0}$, $T_e \geq T_i$ and $\lambda_{De} \gg \lambda_{Di}$ this implies that $\lambda_D \simeq \lambda_{Di}$, means the thickness of sheath is determined by number density and temperature of electrons. If thickness of sheath is

obtained by number density and temperature of electrons then we have, $T_e n_{io} \ll T_i n_{eo}$ and $\lambda_{De} \ll \lambda_{Di}$ this implies that $\lambda_D \simeq \lambda_{De}$.

1.3.3 Characteristics Frequency

Perturbations of plasma ingredients from their equilibrium positions, assembled a space charge field in such a direction to maintain the neutrality of the plasma by dragging the particles back to their novel positions. Due to rioting of their inertia, they will exceed and will be again dragged back to their original positions by the space charge field of the reverse polarity. Hence, they continuously keeping oscillation about their equilibrium position with a specific frequency called plasma frequency. Complex plasma contains electron ions and dust particles. The electrons oscillate around ions, ions oscillate around dust particles and dust particles oscillate around their equilibrium position with corresponding frequencies $\omega_{pe} = \left(\frac{4\pi n_{ee} e^2}{m_e}\right)^{\frac{1}{2}}$, $\omega_{pi} = \left(\frac{4\pi n_{ie} e^2}{m_i}\right)^{\frac{1}{2}}$, and $\omega_{pd} = \left(\frac{4\pi n_{do} Z_d^2 e^2}{m_d}\right)^{\frac{1}{2}}$ respectively.

1.3.4 Coulomb Coupling Parameter

It is a distinctive property of a dusty plasma obtained by taking ratio between dust potential energy and thermal energy and used for the formation of dusty plasma crystals.

Mathematically it is given as,

$$\Gamma_c = \frac{Z_d^2 e^2}{a K_B T_d} e^{-\frac{a}{\lambda_D}} \quad (1.5)$$

Here T_d is the dust temperature, and K_B is the Boltzman constant. Its numerical value decides about the weakly and strongly coupled dusty plasma. If $\Gamma_c \ll 1$ then dusty plasma is weakly coupled while for strongly coupled $\Gamma_c \gg 1$.

1.3.5 Charging Mechanisms

There exists different procedures for charging of dust particles. The charge on dust particles will be either positive or negative depends upon their charging mechanisms. In

space and astrophysical plasmas, the dust particles develop charged by photoionization or radioactive decay process whereas in laboratory dusty plasmas electron bombardment is the traditional means for charging dust particles. In case of photoionization method, the dust particles gain positive charge because the electrons are emitted by the dust grains while the Radioactive decay they become negatively charged [16]. Generally, electrons and ions are considered as a plasma particles. When dust particles are injected in plasma then they interact with electrons and ions. As electrons are energetic than ions then probability of interaction of dust with electrons rather than ions is maximum hence they get negative charge having negative potential. Similarly, interactions with ions make dust particles positive charge with positive potential [17]. The equilibrium is achieved when concentration of ions and electrons become equal. The charge on dust grain is determined by $\frac{dq}{dt} = \sum I$. The electron current is repulsive while ions current is attractive type current, and at symmetry the net current flowing is zero i.e. $\sum I = 0$.

The dust particle obtained positive charge by photoemission (by incidence of a flux of ultraviolet (UV) photon, the emission depends upon intensity of radiations falling on dust grain), thermionic emission (dust surrounding is heated by hot filament or by high intense laser or infrared radiations). [18]. When highly energetic electron interacts with dust particle then there are two possibilities i.e. it may stick with dust particle or cause knocking of secondary electron by transferring of its whole energy. This fully transfer of energy result emission of secondary electron. Hence dust particle becomes positive charge. This termed as electron impact [19]. Beside these an important method usually used for dust charging is called field emission method. It occurs at a surface electric field of 10^6 v/cm when we provide very high potential [20].

1.4 Occurrence of dusty plasma

Dusty plasma occurs naturally and can be produced in laboratory because it is a hastily rising field of research which includes vital problems in the physics of plasmas, such as hydrodynamics, kinetics of phase changes, nonlinear physics, solid state physics and

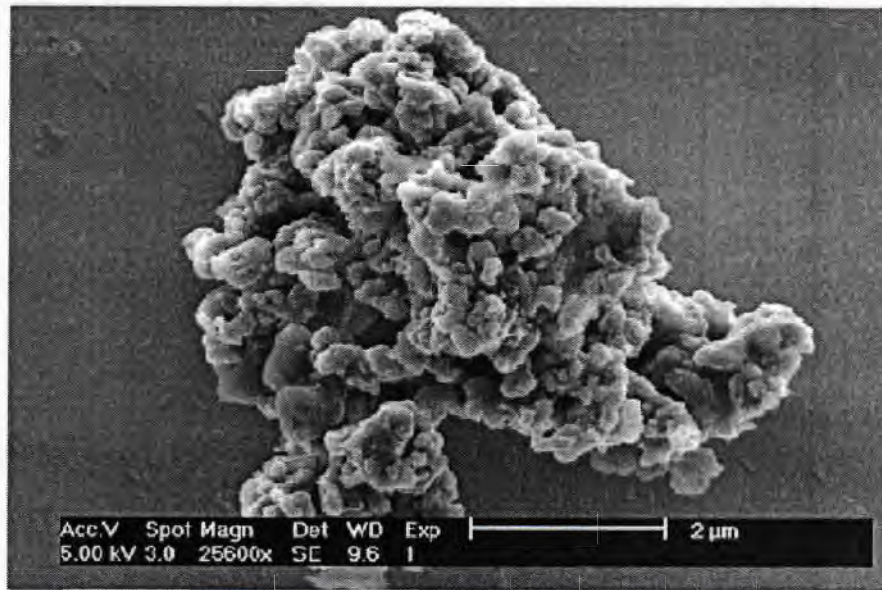


Figure 1.3: An image of inter-planetary dust [24].

numerous applications in nano and plasma technologies [21].

1.4.1 Interplanetary space

The advocater of dust in solar system is Hannes Alfvén. The physical parameters (mass, density, charge) etc. be contingent upon their source and environment. The presence of interplanetary dust is due to reflection of sun light from cosmic dust which is visible before sun rise and after sunset. The asteroids are other important cause of dust collision among asteroids also produce dust [22]. The formation of new planets and comets is due to clotting of this dust. It has been observed by NASA that nearly 40000 tones dust (having size 5-20mm) from interplanetary space is deposit at a height of 10 – 18km on earth per year. For this purpose a collector is used. The dust particles were observed at plastic plates. These dust particles are so brittle and breakable. After hitting collector surface they breaks into several fragments. Obviously, they are rich in carbon, mineral grains and interstellar silicates. The characteristics parameters of dusty plasma are $n_d \simeq 10^{-12} \text{cm}^{-3}$, $T_e \simeq 10^5 \text{K}$, $r_d = 2 - 10 \mu\text{m}$ and $\frac{a}{\lambda_D} \simeq 5$ [23]. Planetary dust is shown in Fig. 1.3.

1.4.2 Planetary rings system

The Saturn rings was discovered by Galileo in 1610, as shown in Fig. 1.4. The rings A and B are separated by Cassini Division. The particles in these rings are mostly of ice having size from microns to meters. The utmost fascinating features detected in Saturn's ring is the radial spokes. If R_s is the radius of Saturn then these spokes are confined innermost edge kept at $1.52 R_s$ while external edge at $1.95 R_s$ Smith *et al.* [25, 26].

The scattering of light from these spokes show that these spokes consist of dust with size $0.5\mu m$. A periodic stream of dust has been detected by spacecraft Ulysses. This spacecraft was used by European space agency in 1992 especially for detection of dust. It was well equipped with dust detector and a distance of 1AU from Jupiter this space craft recorded streams of dust coming from Jupiter [27]. Jupiter ring system was revealed by Voyager 1 and Voyager 2 by taking images, while Voyager 2 take its complete set of fine images. It is comprising of three major rings. The dust particulates exist in Jupiter moons named Adrastea and Metis. The Uranus has nine rings beside these the Voyager spacecraft discovered further rings named as 1986U1R and 1986U2R and exposed that these rings are bounded by belt of fine dust particles. The dust particles having radius $1.6 - 10 \mu m$ composed of material of dirty ice or silicates also observed in Neptune rings system. These dust particle produce noise with frequency $10Hz - 100KHz$. The Uranian ring system was explored in 1970 and Voyager spacecraft had taken image of its ring system in 1986. It has nine rings beside these the Voyager spacecraft discovered further rings named as 1986U1R and 1986U2R and exposed that these rings are bounded by belt of dust particles [28].

1.4.3 Earth's atmosphere

At a height of 80-90 km from earth there exist location of polar summer mesopause (PSMp), and it is observed by Cho and Kelley [30]. These (PMS) cause formation of a typical form of clouds called Noctilucent clouds (NLCs) [31]. The main source of dust



Figure 1.4: An image of Saturn's rings, taken by spacecraft [29].

in these regions is man-made pollution, in the form of rocket exhausts. The dust in the form of Al_2O_3 with having size $1 - 10 \mu m$ observed by [32]. A population of smoke particles also exists above (PSMp) and NLCs (as shown in Fig. 1.5) due to burning of meteoroids. Metallic and silicate dust grains with radii of few *nanometers* are also observed in this smoke.

The laboratory dusty plasmas are different from astrophysical dusty plasmas. Actually laboratory dusty plasma has geometric boundaries whose assembly, preparation, temperature and conductivity effect the development and transport of the dust particles. The boundary conditions can easily be applied and it is used widely in industries [34]. The Glow discharges [35], Q-machines [36], rf discharges [37], DC discharge plasma devices are used for the production and dynamic study of dusty plasma.

1.5 Applications of dusty plasma

Dusty plasma has vast applications in various fields of sciences. For the case of material science (nanotechnology, semiconductor industry) it is used in growth of nano-crystals such as silicon [38], coating and depositions of thin films [39], powder formation, manufacturing of microchips and for synthesis of materials. It is observed that their life time,



Figure 1.5: A view of Notilucent clouds after sunset [33].

efficiency, chemical and physical properties increases by using dust grains of very small sizes. The early problem concerning with silicon wafer is solved by using dust particles. There were unwanted pollution on the surface of silicon. By placing sub-micron particles it is investigated that grip of film and formation of cavities reduces.

The radio isotopes such as Pu^{238} , Po^{210} , Ur^{235} and Sr^{90} are used for nuclear medicines and as a fuel of power stations. These sources are less efficient. For solid and efficient isotopes, the mixture of gas and dust can be used. In nuclear photovoltaic battery radioactive dust particles are used. The schematic diagram is shown in Fig. 1.6. These dust particles increase the efficiency from 25 – 35%, [40]. Beside this we are familiar that in fusion devices dusty plasma exists. It is considering as a harmful, and some consequences are considered useful. Dust particles wander here and there after formation, if tritium exist with dust, then it cannot be purified and dust become carrier of this cause problem. They become so reactive that presence of some hydrogen caused explosion or leakage of coolant [41]. There exist many challenges exposed by the fusion science community, linking to presence of dust because it changes the plasma behavior and cause engineering issues in fusion devices [42]. These are found at the bottom of fusion devices where they can block the spacing and filled gaps [43].

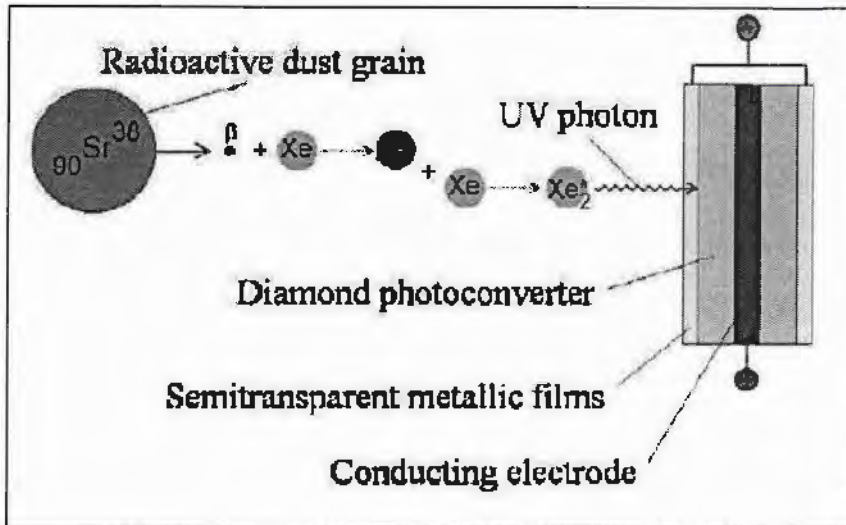


Figure 1.6: Figure of an photovoltaic source of electric energy, in which dust particles are used [44].

1.6 Maxwellian and non-Maxwellian distribution functions

1.6.1 Maxwellian Distribution Function

Maxwellian distribution is an exceptional distribution function that is used for a gas when the gas molecules are in thermal equilibrium but having different velocities. The most probable distribution for this system is given by James Clerk Maxwell in 1800. In three-dimensional case, this distribution is given as

$$f_s(v) = n_s \left(\frac{m_s}{2\pi K_B T_s} \right)^{\frac{3}{2}} \exp\left[-\frac{m_s v^2}{2K_B T_s}\right] \quad (1.6)$$

Here $f_s(v)$ is distribution function, n_s , m_s , and T_s are the number density, mass and temperature of the gas molecules of type s , respectively. The K_B is Boltzman constant while v , is speed of gas molecules. This distribution function as shown in Fig. 1.7, is used for that system which will be in thermodynamic equilibrium.

The number density of particles is obtained by integrating Eq (1.6) for all velocities



Figure 1.7: The Maxwellian velocity distribution [45].

$$\int_{-\infty}^{+\infty} f_s(v) dv_x dv_y dv_z = n_s \quad (1.7)$$

The plot of Maxwellian Distribution as shown in Figure 1.7. Where $v_p = \sqrt{\frac{2K_B T_s}{m_s}}$, $v_{avg} = \sqrt{\frac{8K_B T_s}{\pi m_s}}$, and $v_{rms} = \sqrt{\frac{3K_B T_s}{m_s}}$ are the most probable, average and root-mean square speeds of the particles of type s . Area under the curve give us total number of particles. As we consider plasma as a quasi-neutral gas then at thermodynamic equilibrium the distribution function for each species of plasma will be Maxwell distribution function [46].

1.6.2 Non Maxwellian Distribution Functions

The presence of non-thermal particles is observed in laboratory and space plasma. These non-thermal particles are high energetic and become more significant then we cannot use Maxwellian distribution because Maxwellian distribution is not realistic in all conditions. In different plasma atmospheres such as auroral ionosphere, magnetotail, Earth's bow shock as well as in the laboratory, two different inhabitants of electrons (hot and cold) have been observed [47]. In the Earth's magnetosphere and solar winds the occurrence of extremely energetic electrons with non-Maxwellian distribution have also been observed [48]. From past few years a number of researcher organized

theoretically and experimentally with non-Maxwellian behavior of energetic particles.

Different distributions functions for space plasma having super-thermal species or other eccentricity from pure Maxwellian behavior have become the utmost prevalent field from past few years due to its vast applications in laboratory and astrophysical plasma [49]. Non-thermal plasma can be useful to endorse chemical reactions at minor functional temperature ranges where a predictable substance cannot be used. The interest is growing in the generation of non-thermal plasma at laboratory level for an extensive diversity of applications in astrophysics. The super-thermal ions and electrons observed in interplanetary medium, which delivers evidence about their sources. In production of plasma by laser the super-thermal particles are also observed [50].

The presence of such particles revealed an affected change in plasma topology. There exists a lot of literature in which scientist study the effect of super thermal particles in simple and multi component plasma on linear and nonlinear waves, acoustic like solitary waves, drift waves, ion acoustic solitons and super solitons, as well as their effect on charging of dust species, and dust acoustic solitons,[51].

We in this thesis give some detail of Non- Maxwellian distribution function.

Cairns Distribution

The Cairns non-thermal distributions were first introduced by Cairns *et al.* [52]. Actually, it describes the super thermal particle distribution function which is given by

$$f_e(v) = \frac{n_{eo}}{(3\alpha + 1)\sqrt{2\pi v_e^2}} \left(1 + \frac{\alpha v^4}{v_e^4}\right) \exp\left(-\frac{v^2}{2v_e^2}\right) \quad (1.8)$$

Here v_e is thermal velocity and n_{eo} is the equilibrium density of electron. The term α is non-thermal parameter. When $\alpha \rightarrow 0$ distribution function become Maxwellian. Integrating this distribution function over all microscopic velocities, the number density of electrons can be written as

$$n_e = n_{eo}[1 - \beta\phi + \beta\phi^2] \exp[\phi] \quad (1.9)$$

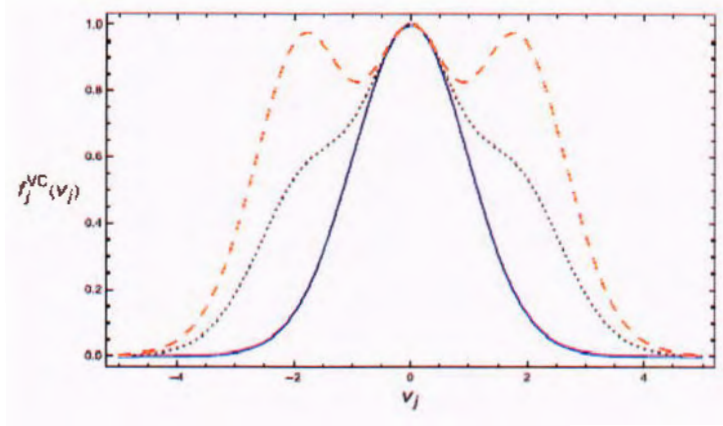


Figure 1.8: The Cairn's distribution function for different values of α [53]

Where $\beta = \frac{4\alpha}{1+3\alpha^2}$, and ϕ is the normalized electrostatic potential i.e. $\phi = \frac{e\phi}{K_B T_e}$. It is predicted that the occurrence of non-thermal electrons can change the nature of ion solitary structure, producing non-linear solitary waves with useless density. The Cairns distribution for different values of α , is shown in Fig.1.8.

In different space plasma atmosphere, the plasma species [54] are not in thermal equilibrium. There exists a lot of literature in which different scientist use Cairns distribution function for these non-thermal species. For the case of non-uniform plasma A. Mushtaq and Shah [55] study the solitary waves and vortices caused by sheared-flow with non-thermal electrons. Dust-acoustic solitons electron solitary waves, ion acoustic solitons, electrostatic solitary structure in dusty plasma, and ion-acoustic vortices, has been observed, in different plasma regimes with cairn distribution function [56].

Non-Extensive Tsallis Distributions

The energy and entropy of the system are considered as extensive variables in statistical mechanics. Its mean that the energy of the system depends upon size of the system. The extensive behavior of energy and entropy is applicable for short range interactions. While for the case of long range interactions, the energy and entropy become non-extensive and, Tsallis [57], gave an idea based on maximum entropy and introduced a new type of non-thermal distribution called q-non-extensive Tsallis distribution. The

distribution function for species j can be written as

$$f_j(v) = C_{qj} (1 - (q - 1) \left(\frac{m_j v^2}{K_B T_j} + \frac{Q_j \phi}{K_B T_j} \right)^{\frac{1}{q-1}}) \quad (1.10)$$

Where C_{qj} is the normalization constant and m_j is the mass of the species. The q ($-1 < q \leq 1$) called entropic index, characterizes the degree of non-extensivity of the system. For $q \rightarrow 1$, the distribution function reduces to Maxwellian. For $q < 1$ and $q > 1$ give information about the probability of high energy states. Integrating the distribution function over all velocity space, the number density in term of normalized potential $\phi = \frac{e\phi}{K_B T_e}$ is given by

$$n_j = [1 - \delta(q_j - 1)\phi]^{\frac{q_j+1}{2(q_j-1)}} \quad (1.11)$$

where δ is the ratio of species temperature to electron temperature. This provides a suitable frame for the examination of many astrophysical systems which can deal with the non-isothermal nature in plasma systems with the Colombian long-range interactions.

From past few decades the q -nonextensive distribution function got great importance for studying the non-Maxwellian plasma systems in different plasma regimes [58]. Different waves such as ion-acoustic solitary wave [59], Langmuir waves [60], *linear and non-linear Landau damping* has been study by different authors in magnetized and non-magnetized *multi-component* plasma. Besides this instability such as Jeans instability, and modulational instabilities, and plasma oscillations [61], has been observed, by using q -nonextensive distribution function.

General (r, q) Distributions

When some characteristics of non-Maxwellian plasma cannot explained by other distributions like kappa distribution then (r, q) is used. It has two spectral indices r and q , and the distribution function is given as

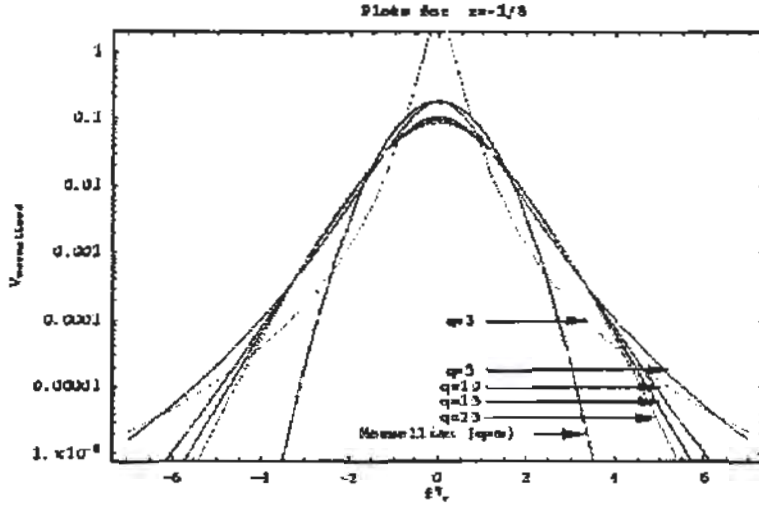


Figure 1.9: A graphical representation of (r, q) for different values of index q and r [63].

$$f(r, q) = \frac{3(q-1)^{-\frac{3}{2}(1+r)} \Gamma q}{4\pi \Psi^3 [q - \frac{3}{2}(1+r)] \Gamma [1 + \frac{3}{2}(1+r)]} \times \left[1 + \frac{1}{q-1} \left(\frac{v^2}{\Psi^2} \right)^{1+r} \right]^{-q} \quad (1.12)$$

Where $v = \sqrt{\frac{T}{m}}$ is the thermal velocity Γ is the gamma function and Ψ is dimensionless function given as,

$$\Psi = v \sqrt{\frac{3(q-1)^{-\frac{1}{2}} \Gamma [q - \frac{3}{2}(1+r)] \Gamma [1 + \frac{3}{2}(1+r)]}{\Gamma [q - \frac{5}{2}(1+r)] \Gamma [\frac{5}{2}(1+r)]}}$$

When $r = 0$, $q \rightarrow \kappa + 1$ and $r = 0$, $q \rightarrow \infty$ it reduces to kappa and Maxwellian distributions respectively. The index q is used for the high-energy tails while r describes sharp top of the distribution function. Thus, this distribution type is more accurate to describe plasma systems containing trapped particles [62]. This distribution function is as shown in Fig. 1.9.

This distribution function has been widely used for studying different waves phenomena in complex and ordinary plasma. Especially the electrostatic modes [64] electromagnetic modes and Langmuir waves [65], has been investigated. Beside this dust charging and trapping of particles [66], and their effect on different waves has been observed by using (r, q) distribution function [67].

1.7 Kappa Distribution

The basic fundamentals of the kappa distribution rises, obviously from non-extensive Statistical Mechanics. For the replacement of Maxwell distribution it is used, when a system is out from thermal equilibrium, frequently found in astrophysical plasmas [68]. The velocity distributions for space plasma particles show (*non – Maxwellian*) superthermal tails, decreasing usually as a power law except exponentially. The Kappa (κ) often called generalized Lorentzian velocity-distribution functions (*VDFs*). This distribution function was used by Vasyliunas [69]

$$f_j^\kappa(r, v) = \frac{n_j}{2\pi(\kappa\omega_{\kappa j}^2)^{\frac{3}{2}}} \frac{\Gamma(\kappa + 1)}{\Gamma(\kappa - \frac{1}{2})\Gamma(\frac{3}{2})} \left(1 + \frac{v^2}{\kappa\omega_{\kappa j}^2}\right)^{-(\kappa+1)} \quad (1.13)$$

Here $\omega_{\kappa j} = \sqrt{\frac{(2\kappa-1)\kappa T_j}{\kappa m_j}}$, m_j , n_j and T_j are the modified thermal velocity, mass, number density and temperature of the particles of species j respectively. κ is called kappa index whose values lies between $(\frac{3}{2}, \infty)$. $\kappa_c = \frac{3}{2}$, called critical value of kappa. If $\kappa \rightarrow \infty$ then it becomes Maxwellians, and system is will be in equilibrium state. The integration of 1.13 over velocity space gives number density,

$$n_j = n_{j0} \left[1 - \frac{e\phi}{(\kappa - \frac{3}{2})K_B T_j}\right]^{-\kappa + \frac{1}{2}} \quad (1.14)$$

In the following space plasma environment, the Kappa (κ) distributed plasma species showing super-thermal tail with $(2 < \kappa < 6)$ has been observed [70, 71].

- Solar winds
- Magnetosphere of planets
- Planets plasma sheet
- Magneto-sheath of radiations belts
- Plasma-sheet of Jupiter
- Magnetosphere of Mercury
- Magnetosphere of Jupiter
- Magnetosphere of Uranus
- Magnetosphere of Neptune

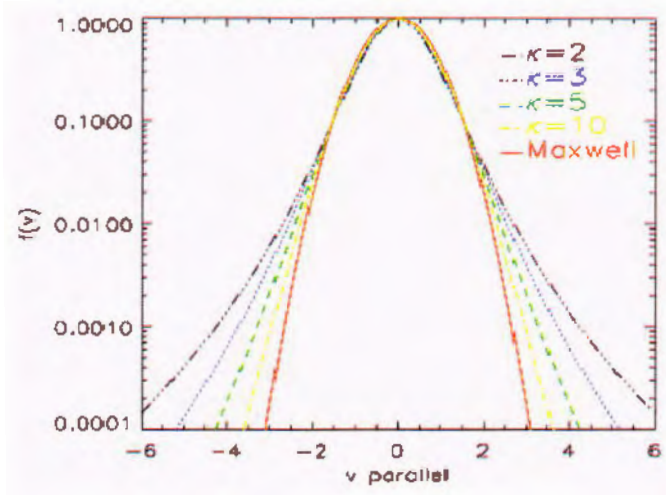


Figure 1.10: Kappa (*VDFs*) for different value of κ [72].

- Magnetosphere of Saturns
- Saturns moon Titan

For different values of kappa the distribution function is as shown in Fig. 1.10.

In above mentioned plasma environment there exists several procedures and tools in which origin existence, impact and features of Kappa-distribution has been studied. Hasegawa *et al.* [73] proposed that by placing plasma in an intense stream of radiations, the velocity an-isotropy, and coulomb field variation cause generation of power law distribution. Non-uniformity [74] and resonance phenomena in whistler waves of solar winds produce super-thermal population of electrons, with high energy tail. Shizgal, [75] investigated that waves with large amplitude are also responsible for plasma species having Lorentzian distribution. Using kappa model for ions-exosphere Pierrard *et al.* [76] and Moore [77], studied the magneto sphere of earth and Saturn's respectively. The isotropic Kappa distribution [78] and anisotropic Kappa distribution [79], has been studied by considering plasma species parameters, like (velocity , temperature) etc. as isotopically and an-isotopically. Figure 1.11, show different some formulation used in space for Kappa.

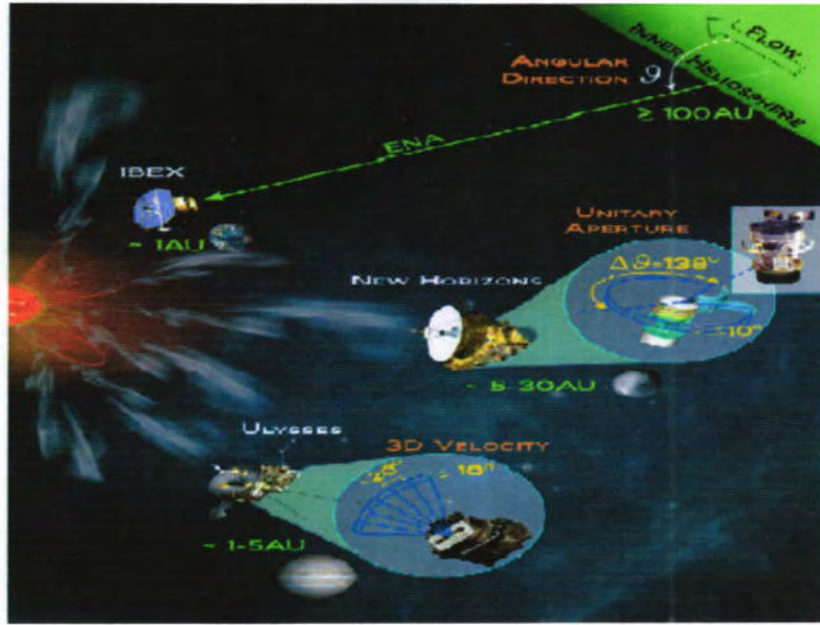


Figure 1.11: A schematic diagram of most common formulations of the kappa distribution for direct use in space plasma analyses [80].

1.8 Waves and Instabilities in Dusty Plasma

1.8.1 Waves in dusty plasma

It is a dynamic area associated with the field of dusty plasma. In the physics of dusty plasma charge on dust is a crucial player. After entry of dust in normal ion-electron plasma dust particulates get charge, by variety of ways as discussed in **charging mechanisms**. This cause non-uniformity, and departure of ion and electrons from quasi-neutrality regime. Then charge dust produce diverse modes of waves [81].

Dust Acoustic waves

In multicomponent collisionless dusty plasma the theoretical prediction of $\check{D}\check{A}W$ s has been given by Rao *et al.* [82], while experimental confirmation by [83]. Due to perturbation the dust grain start oscillation against the quasi-equilibrium. The mass of dust provide inertia to keep oscillation while background electrons and ions provide pressure to sustain the wave. Hence it is analog to ion acoustic wave [84].

The true regime of the DA mode is $V_{thd} \ll \omega/k \ll V_{thi}, V_{the}$. The dispersion relation is given by,

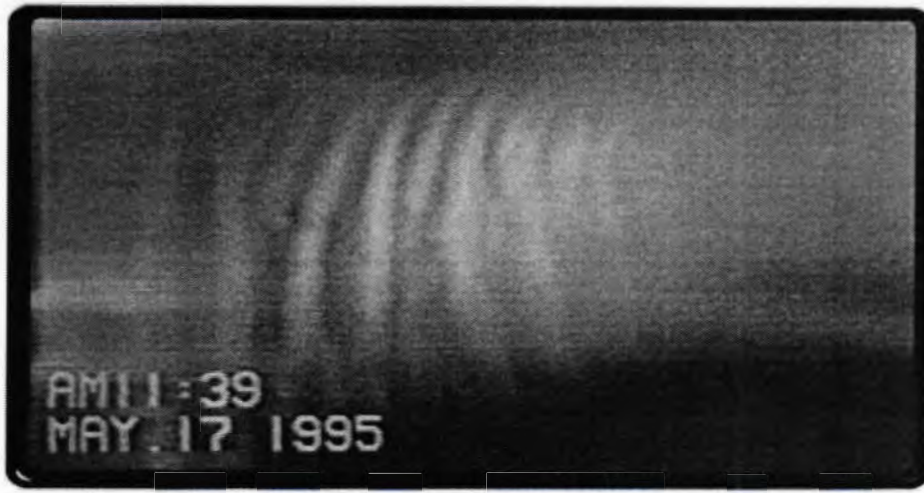


Figure 1.12: An image of a DAWs pattern taken by video camera [87].

$$\omega = \omega_{pd} \left(1 + \frac{\omega_{pe}^2}{k^2 V_{the}^2} + \frac{\omega_{pi}^2}{k^2 V_{thi}^2} \right)^{-\frac{1}{2}} \quad (1.15)$$

Where $\omega_{pe} = \left(\frac{4\pi n_e e^2}{m_e} \right)^{\frac{1}{2}}$, $\omega_{pi} = \left(\frac{4\pi n_i e^2}{m_i} \right)^{\frac{1}{2}}$, and $\omega_{pd} = \left(\frac{4\pi n_d Z_d^2 e^2}{m_d} \right)^{\frac{1}{2}}$. The dust acoustic waves are low frequency waves because the frequency has inverse relation with mass and dust particles are heavier than ions. The typical frequency range of this mode is $(10 \text{ to } 100) s^{-1}$ which makes it predominantly fascinating from the experimental point of view. The several linear and nonlinear features of the different DAWs have been described not only because they exist in both space dusty plasmas [85]. The nonlinear DAWs for different dusty plasma situations have also been rigorously investigated by several authors [86]. The beauty of dust acoustic wave is that its wave fronts video image is possible and they can be seen with naked eyes, the one is shown in Fig. 1.12.

Dust ion Acoustic Waves

The theoretical prediction of low frequency DIAW given by Shukla and Silin [88], experimentally observed by Barkan *et al.* [89] and Nakamura *et al.* [90]. There exist two ways to view DIAW modes. First, mode the inertia is provided by ion (with assumption, stationary dust and $T_i \ll T_e$), and restoring force comes from electrons pressure). Here the true regime of DIA mode is $V_{thi} \ll \omega/k \ll V_{the}$. The dispersion

relation for DIAWs

$$\frac{\omega_{pi}^2}{\omega^2} - \frac{\omega_{pe}^2}{kV_{the}^2} = 1 \quad (1.16)$$

In second way, we incorporate the dynamics of dust and ion particles, then inertia arises from both ion and dust particles, and electrons provide restoring force. The regime of DIA mode is $V_{thd}, V_{thi} \ll \omega/k \ll V_{the}$ and dispersion relation is given by

$$\frac{\omega_{pd}^2 + \omega_{pi}^2}{\omega^2} - \frac{\omega_{pe}^2}{kV_{the}^2} = 1 \quad (1.17)$$

De Angelis *et al.* [91] inspected the propagation of DIAW in a dusty plasma in which a spatial inhomogeneity is formed by a distribution of steady dust particles. The linear properties of the DIAWs are nowadays well established from both theoretical and experimental , point of view. Their phase velocity is larger than dust and ion thermal velocities. The cause, for larger phase velocity of the DIA mode is the declined number density of the electrons [92]. The low-frequency DIAWs in cosmic and Earth's mesosphere atmosphere has been observed. A noise produce by these wave has been observed in Saturn F-rings.

1.8.2 Instabilities in Dusty Plasma

We are familiar that there exists a large free distance between particles of space plasma. Their collision time is very large i.e. they collide once after few days. This plasma is considered out of thermodynamic equilibrium. This mean there exist a lot of free energy which cause instabilities, simply deviation of plasma from thermodynamic equilibrium. This deviation consequences are different waves modes, with exponential growth in amplitudes.

Mathematically, let deviation from thermodynamic equilibrium is x then $x \propto \frac{dx}{dt}$, this implies $x = y \frac{dx}{dt}$, by solving this we get $x = \exp[yt]$. The y called growth rate of instability.

These deviations can be produced by applying external perturbations, in the form of electric field, magnetic field, electromagnetic radiations, or by injection of new plasma

species. Internally violent motion of plasma species, fluctuations in pressure, temperature, and number of particles are responsible for creating instabilities.

The instabilities play a vital role, by releasing free energy it can drag the system into thermodynamic equilibrium. The instabilities can be classified as macro-instabilities and micro-instabilities.

Microinstability

The cause of microinstability is velocity space anisotropy in the plasma or in simple words distribution of velocity other than Maxwellian. A significance of a microinstability is a greatly improved level of variations in the plasma associated with the unstable mode. These variations are called microturbulence. Microturbulence can lead to higher radiation from the plasma and to higher scattering of particles resulting in irregular transport coefficients, e.g. irregular electric and thermal conductivities. The following instabilities are microinstabilities.

- Beam driven instability
- Electrostatic instability
- Electromagnetic instability
- Mirror instability

Macroinstability

The deviation of plasma from thermodynamic equilibrium by confining in space with a locally higher or lower thermodynamic quantities such as density, temperature, pressure etc. or convectively unstable system called macroinstability. The macroinstability occurs in low frequency regime. The following instabilities are macroinstabilities [93].

- Ballooning instability
- Drift waves instabilities
- Rayleigh Taylor instability
- Current pinch instability
- Kelvin Helmholtz instability

TH: 18071

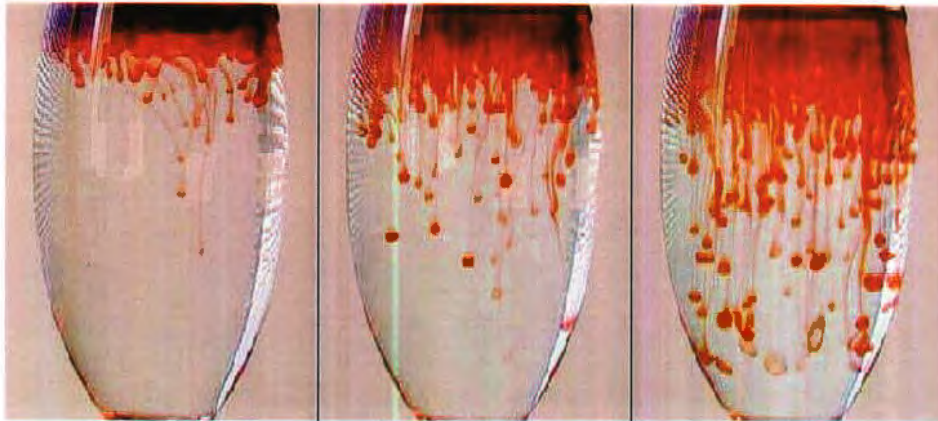


Figure 1.13: An image of *RT instability*, where heavy fluid is supported by lighter fluid [96].

Rayleigh Taylor Instability

The Rayleigh–Taylor instability, is an instance of macroscopic instability rising from plasma inhomogeneities generally based on fluid or MHD model of plasma. It is experimentally investigated by Taylor and Lewis, and theoretically by Lord Rayleigh's [94].

In plasmas, a Rayleigh Taylor instability as shown in Fig. 1.13, can arise when a heavier fluid is supported by lighter fluid. The examples of *RTI* are water postponed above oil in the gravity of Earth, a large cloud of rubble and dust shaped like a mushroom from volcanic explosions and atmospheric nuclear explosions, supernova bursts in which mounting central gas is accelerated into denser shell gas, instabilities in plasma fusion reactors and inertial confinement fusion [95].

1.9 Kelvin Helmholtz Instability

The Kelvin-Helmholtz (K-H) primarily studied, theoretically by Hermann von Helmholtz in 1868 and Lord Kelvin in 1871 [97]. This instability can arise when there is velocity shear in a solitary perpetual fluid or there exist a velocity fluctuation across the crossing point between two fluids. For the situation of a conductive, magnetized incompressible fluid, the instability has been investigated by Chandrasekhar. The instability norms for a fluid flowing along the direction of the magnetic field is that the comparative

speed between two adjacent layers surpass the root-mean-square Alfvén speed in the two layers [98]. Blowing of winds on the water surface and on the clouds, generates waves, are the classical examples of KH instability [99].

Actually, sheared flow is the main player in this instability. This also occurs in solar winds, cometary tails, stellar medium magneto-spheres and in polar cusps [100]. It has been investigated with the help of viscous model that in these environment K-H instability produces by the plasma sheared flow [101]. The Kelvin-Helmholtz instability renovates the energy of plasma into other forms such as kinetic energy and magnetic energy, and the disorder formed by this instability is a significant cause of viscosity. Beside this injection of a jet of fluid into stagnant fluid is another example of this instability. Where jets kinetic energy is a source for creating turbulence, in fluids flow, hence instability rises. These jets are observed in several astro-physical atmospheres.

In a magnetized dusty plasma this instability is investigated by [102]. It may occur in dusty plasma due to sheared flow or when adjacent layers are in relative motions. We can consider dust as stagnant or by incorporating dust dynamics, in both cases K-H instability is produced [103]. If U_1, ρ_1 and U_2, ρ_2 be the velocities and densities of upper and lower dusty plasma fluids respectively as shown in fig 1.14, then due to sheared flow at the interface of these fluids K-H modes arises, with dispersion law [104],

$$\left(\omega_{KH}^2 - k_{\perp} \frac{\rho_1 U_1 + \rho_2 U_2}{\rho_1 + \rho_2} \right)^2 = \frac{gk(\rho_1 - \rho_2)}{\rho_1 + \rho_2} + \frac{2k_{\perp}^2 B_o^2}{\mu_o(\rho_1 + \rho_2)} - \frac{k_{\perp}^2 \rho_1 \rho_2 (U_1 - U_2)^2}{(\rho_1 + \rho_2)^2} \quad (1.18)$$

Then criteria for instability is

$$\rho_1 + \frac{2k_{\perp}^2 B_o^2}{gk\mu_o} < \frac{k_{\perp}^2 \rho_1 \rho_2 (U_1 - U_2)^2}{gk(\rho_1 + \rho_2)} \quad (1.19)$$

Eq1.19 reveals that magnetic field have a tendency to stabilize the mode and kinetic energy between the two fluids is destabilizing. If number densities and masses of fluids are equal then K - H instability can also occur except Alfvén speed $V_A < \left(\frac{U_1 - U_2}{2} \right)$. If both fluids are neutrals then the possible condition for K - H instability is

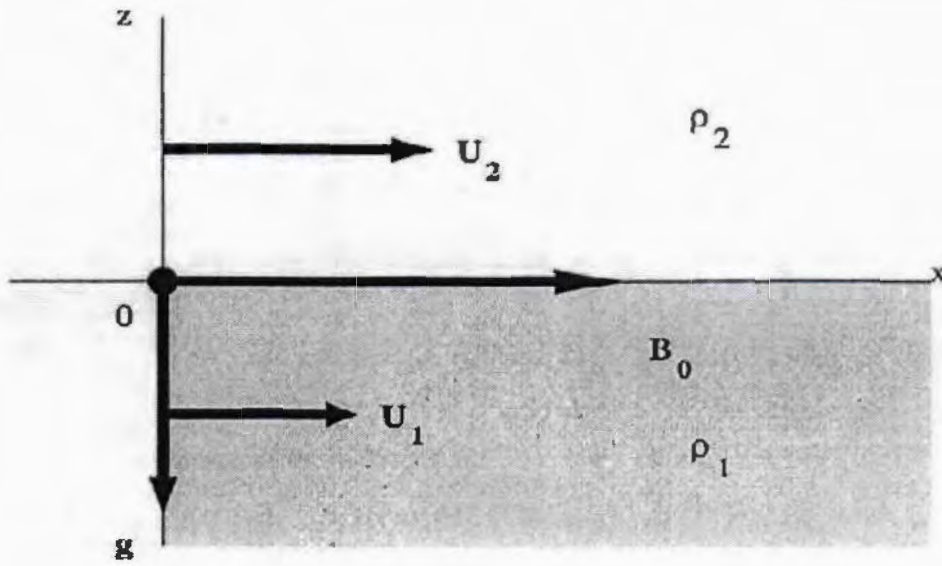


Figure 1.14: Configuration for the *Kelvin – Helmholtz* instability [105].

$$\rho_1 < \rho_2 + \frac{k_{\perp}^2 \rho_1 \rho_2 (U_1 - U_2)^2}{gk(\rho_1 + \rho_2)} \quad (1.20)$$

The *Kelvin – Helmholtz instability* is most important in dusty plasma for the proper understanding of space plasma as well as in laboratory where sheared dust flow obviously occurs [106]. Li Lu *et al.* [107] observed the damping and growth modes of K- \hat{H} instability in magnetized dusty plasma caused by dust sheared flow. Similarly in the regime of weakly coupled, strongly coupled, magnetized, and un-magnetized, dusty plasma K- \hat{H} instability has been studied by number of authors.

1.10 Layout of Thesis

The main concern of this thesis is about the theoretical and numerical study of K-H modes in dusty plasma with Kappa distribution. The first chapter is about introduction of dusty plasma, its occurrence in space and laboratory, and its vital applications. Beside this we discuss instabilities and different waves such as DAW, DIAW's in dusty plasma, Maxwellian and non-Maxwellian plasma. The chapter 2 is about the theoretical and analytical study of K-H modes in dusty plasma with non-Maxwellian electrons i.e. kappa distributed electrons. We obtained relations of frequency and growth rate.

On the behalf of these relations and using the numerical data of Saturn's rings we discussed our results. While in final chapter we summarized our work and sum up the important conclusion of whole thesis.

Chapter 2

Kelvin Helmholtz Instability in Dusty Plasma with Kappa Distributed Species

2.1 Introduction

Dust is most prevalent constituent of the Universe. The dust particulates are round or irregularly shaped particulates of carbon, silicate or other material. Beside this they may be composed of ice or tiny liquid droplets [108]. Dust particle after entering in plasma get charge both positive and negative hence termed as four component dusty plasma. The dust particles with opposite polarity has been observed in earth mesosphere, comet, and cometary tails etc. as well as in laboratory devices [109]. Dynamic properties of dusty plasma with opposite polarity has been examined theoretically and experimentally [110].

Throughout from the previous few spans the study of dusty plasmas is a fast-growing area of research. The propagation of wave and instabilities in this plasma have established a significant attention due to some space observations [111] as well as experimental endorsement [112]. The electrostatics waves with different modes such as (Langmuir modes, DIA modes, and DA modes) [113] and EM-waves, develop an interest for study of waves in dusty plasmas . With the help of different fluid models, by using

different simulation techniques, the propagation, damping and numerous dispersion properties of these waves, has been studied by Li *et al.* and Shukla [114, 115]. Actually, a suitable platform, for different waves and instabilities in dusty plasma is provided by polarity effect. The positive and negative charge dust are variable parameters in dusty plasma. There exist numerous kinds of hydrodynamic, kinetic and MHD instabilities in dusty plasma [116].

Hartquist *et al.* [117] used a kinetic treatment for the study of streaming instabilities in a cometary atmosphere, there exist a relative drift between cometary dust and the solar wind plasma flow. It was observed that an instability, required small dust velocity distribution and the existence of an appropriately high neutral density that can reduce the instability due to ion neutral or electron neutral collisions. Two stream instabilities in an un-magnetized dusty plasma is studied by Bharuthram *et al.* [118], they observed the impact of charge of dust on growth rate and drift speed. The Rayleigh-Taylor instability in dusty plasma was study by D'Angelo [119], result shows that negatively charged dust significantly decreases the range of unstable wave numbers, and vice versa. For stagnant dust wave frequencies was much larger than the charging frequency of the dust. Self-consistent charge variations coupled to dust dynamics impact the Rayleigh-Taylor instability [120], important to a quick decrease of the instability regime. Varma and Shukla [121] illustrated straight respond of dust particles to gravity, in Rayleigh-Taylor instability. They also observed that stagnant dust particles reduce not only the growth of this instability, but also the frequency of convective cells. Two stream instabilities and its importance in space plasma especially in rings of Saturn's and different applicable features has been discussed. The Kelvin-Helmholtz instability in magnetized dusty plasma, caused by dust sheared flow for the first time observe theoretically by D'Angelo and Song [122], and experimentally Luo *et al.* [123].

This instability is very important for the study of wave like phenomena in astrophysical plasma as well as in laboratory. Rawat and Rao [124], discussed the positive and negative dust sheared by incorporating dust dynamics. If dust flow is parallel or perpendicular to the applied magnetic field then K-H instability in both cases may oc-

these equations are given as

$$\frac{\partial n_{dj}}{\partial t} + \nabla \cdot (n_{dj} \mathbf{v}_{dj}) = 0 \quad (2.1)$$

$$m_{dj} n_{dj} \left(\frac{\partial}{\partial t} + (\mathbf{v}_{dj} \cdot \nabla) \right) \mathbf{v}_{dj} = q_{dj} n_{dj} (\mathbf{E} + \mathbf{v}_{dj} \times \mathbf{B}) - \nabla P \quad (2.2)$$

where q_{dj} , m_{dj} , n_{dj} and \mathbf{v}_{dj} are electrostatic charge, mass, number density and streaming and fluid velocity of the dust species respectively. Here $j = \pm 1$, for positive dust particle $j = +1$ and for negative dust particle $j = -1$, $\mathbf{E} = -\nabla\phi$ is the electric field with ϕ being the electrostatic potential. In the Eq. (2.2) $\nabla P = K_B T_{dj} \nabla n_{dj}$ is the gradient of pressure, and ∇n_{dj} is the density gradient of the dust species exist in the negative x direction. For the unperturbed density distribution we assume

$$n_{odj}(x) = n_{odj} e^{-\lambda x} \quad (2.3)$$

where λ is in-homogeneity scale length, Consider zero order state, in which

$$\mathbf{v}_{odjx} = 0, \quad \mathbf{v}_{odjy} = \text{constant}, \quad \mathbf{v}_{odjz} = \mathbf{v}_{odjz}(x) \quad (2.4)$$

$$\nabla\phi_o = \left(\frac{\partial\phi_o}{\partial x} \right) \hat{x}, \quad \text{and} \quad \left(\frac{\partial\phi_o}{\partial y} = 0 = \frac{\partial\phi_o}{\partial z} \right) \quad (2.5)$$

Obviously we included $\left(\frac{\partial\phi_o}{\partial x} = 0 \right)$ in the absence of electric field. For equilibrium state, the equation of motion and continuity will be given as

$$m_{dj} n_{odj} \left(\frac{d \mathbf{v}_{odj}}{dt} + (\mathbf{v}_{odj} \cdot \nabla) \mathbf{v}_{odj} \right) = q_{dj} n_{odj} (\mathbf{E} + \mathbf{v}_{odj} \times \mathbf{B}) - \nabla P \quad (2.6)$$

$$\frac{\partial n_{odj}}{\partial t} + \nabla \cdot (n_{odj} \mathbf{v}_{odj}) = 0 \quad (2.7)$$

By putting the value from Eq.(2.4) and Eq.(2.5), in Eq.(2.6) we have

$$-\lambda \mathbf{V}_{thd}^2 + \frac{q_{dj}}{m_{dj}} \left(\frac{\partial\phi_o}{\partial x} \right) - \omega_{odj} \mathbf{v}_{odjy} = 0 \quad (2.8)$$

where $V_{thd} = \sqrt{\frac{K_B T_{d1}}{m_{d1}}}$ is the dust thermal velocity. $\omega_{cd1} = \frac{Z_{d1} e B}{m_{d1}}$ is the dust cyclotron frequency with $q_{d1} = Z_{d1} e$. Z_{d1} is the number of charges residing on dust grains and $\lambda = \frac{\nabla n_{cd1}(x)}{n_{cd1}}$. The density, velocity and potential in perturbed state with time variation can be written respectively as

$$\begin{aligned} n_{1d1} &= n_{1d1}(x, y, z) \exp -i\omega t \\ \mathbf{v}_{1d1} &= \mathbf{v}_{1d1}(x, y, z) \exp -i\omega t \\ \phi_1 &= \phi_1(x, y, z) \exp -i\omega t \end{aligned} \quad (2.9)$$

Consider waves are propagating along y and z - axis i.e.

$$\vec{k} = (k_y \hat{y} + k_z \hat{z})$$

Then the amplitude of the physical perturbed variables in Eq.(2.9) as the function of space and can be written as

$$\begin{aligned} \tilde{n}_{1d1}(x, y, z) &= N_{1d1}(x) e^{i(k_y y + k_z z)} \\ \mathbf{v}_{1d1}(x, y, z) &= \mathbf{v}_{1d1}(x) e^{i(k_y y + k_z z)} \\ \phi_{1d1}(x, y, z) &= \phi_1(x) e^{i(k_y y + k_z z)} \end{aligned}$$

For the study of K-H instability, the system is electrostatically perturbed and fluid wise considered to be linearized. Linearizing equation of continuity and equation of motion by putting $n_{d1} = n_{cd1} + n_{1d1}$ and $\mathbf{v}_{d1} = \mathbf{v}_{cd1} + \mathbf{v}_{1d1}$, then applying Fourier transformation i.e. ($\nabla = ik$, $\frac{\partial}{\partial t} = -i\omega_j$) they can be given as respectively,

$$-i\omega_j n_{1d1} + ik \cdot [(n_{cd1} \mathbf{v}_{1d1} + n_{1d1} \mathbf{v}_{cd1})] = 0 \quad (2.10)$$

$$m_{d1} n_{cd1} [(-i\omega_j) \mathbf{v}_{1d1} + (\mathbf{v}_{1d1} \cdot ik) \mathbf{v}_{cd1} + (\mathbf{v}_{cd1} \cdot ik) \mathbf{v}_{1d1}] + K_B T_{d1} ik n_{1d1} + iq_{d1} (n_{cd1} k \phi_1 + n_{1d1} k \phi_o)$$

different simulation techniques, the propagation, damping and numerous dispersion properties of these waves, has been studied by Li *et al.* and Shukla [114, 115]. Actually, a suitable platform, for different waves and instabilities in dusty plasma is provided by polarity effect. The positive and negative charge dust are variable parameters in dusty plasma. There exist numerous kinds of hydrodynamic, kinetic and MHD instabilities in dusty plasma [116].

Hartquist *et al.* [117] used a kinetic treatment for the study of streaming instabilities in a cometary atmosphere, there exist a relative drift between cometary dust and the solar wind plasma flow. It was observed that an instability, required small dust velocity distribution and the existence of an appropriately high neutral density that can reduce the instability due to ion neutral or electron neutral collisions. Two stream instabilities in an un-magnetized dusty plasma is studied by Bharuthram *et al.* [118], they observed the impact of charge of dust on growth rate and drift speed. The Rayleigh-Taylor instability in dusty plasma was study by D'Angelo [119], result shows that negatively charged dust significantly decreases the range of unstable wave numbers, and vice versa. For stagnant dust wave frequencies was much larger than the charging frequency of the dust. Self-consistent charge variations coupled to dust dynamics impact the Rayleigh-Taylor instability [120], important to a quick decrease of the instability regime. Varma and Shukla [121] illustrated straight respond of dust particles to gravity, in Rayleigh-Taylor instability. They also observed that stagnant dust particles reduce not only the growth of this instability, but also the frequency of convective cells. Two stream instabilities and its importance in space plasma especially in rings of Saturn's and different applicable features has been discussed. The Kelvin-Helmholtz instability in magnetized dusty plasma, caused by dust sheared flow for the first time observe theoretically by D'Angelo and Song [122], and experimentally Luo *et al.* [123].

This instability is very important for the study of wave like phenomena in astrophysical plasma as well as in laboratory. Rawat and Rao [124], discussed the positive and negative dust sheared by incorporating dust dynamics. If dust flow is parallel or perpendicular to the applied magnetic field then K-H instability in both cases may oc-

cur with different growing and damping modes, in low beta plasma [125]. For parallel K-H instability in dusty plasma it is observed that, adiabatic pressure of dust affect the growth rate. While for the case variable dust charge reduction in sheared flow is observed.

There exist a lot of literature in which scientist studied the wave and instability in plasma by considering Lorentzian distributed (Kappa Distribution) plasma species. Shah *et al.* studied ion acoustic shock waves in e-p-i plasma with kappa distributed electrons and positron. The Zaheer and Murtaza [126] studied the Weibel instability in plasma by using kappa distribution. Qureshi *et al.* [127] studied the Langmuir waves and observed that these wave modes become much larger for Lorentzian plasma. The characteristics of ion-acoustic solitary waves, by assuming Kappa-distributed electrons observed by [128]. A relative study about DIA waves, and DA waves in Maxwellian and Kappa-distributed plasmas is given by Zaheer *et al.* [129]. The Lee [130] proposed that dust species are dependent of Kappa index.

We in this thesis are studying the electrostatic K-H modes by using the D , Anglo approach [131], in three component dusty plasma with polarity and Non-Maxwellian effects. Linear dispersion relation is derived and from there both real frequency and growth rate of K-H mode are analyzed. The effect of Kappa distributed electrons, dust polarity and magnetic field are investigated rigorously.

2.2 Basic Formulation

Consider a three component dusty plasma, in which different layers are in relative motion, the dust sheared is the main player for developing KH instability. Let \mathbf{B} is the strength of external magnetic field, which is directed along z-axis i.e. $\mathbf{B} = (0, 0, B\hat{z})$. We assume low β plasma *i.e* the ratio between kinetic and magnetic pressure is small ($\beta = \frac{2\mu_0 n_{d_j} K_B T_{d_j}}{B^2} \ll 1$ approximation). Where μ_0 is magnetic moiment, K_B IS Boltzman constant and T_{d_j} is the dust temperature.

For the analysis of the Kelvin-Helmholtz instability in a dusty plasma, we initiate our work with the help of equations of continuity and momentum. For dust species

these equations are given as

$$\frac{\partial n_{dj}}{\partial t} + \nabla \cdot (n_{dj} \mathbf{v}_{dj}) = 0 \quad (2.1)$$

$$m_{dj} n_{dj} \left(\frac{\partial}{\partial t} + (\mathbf{v}_{dj} \cdot \nabla) \right) \mathbf{v}_{dj} = q_{dj} n_{dj} (\mathbf{E} + \mathbf{v}_{dj} \times \mathbf{B}) - \nabla P \quad (2.2)$$

where q_{dj} , m_{dj} , n_{dj} and \mathbf{v}_{dj} are electrostatic charge, mass, number density and streaming and fluid velocity of the dust species respectively. Here $j = \pm 1$, for positive dust particle $j = +1$ and for negative dust particle $j = -1$, $\mathbf{E} = -\nabla\phi$ is the electric field with ϕ being the electrostatic potential. In the Eq. (2.2) $\nabla P = K_B T_{dj} \nabla n_{dj}$ is the gradient of pressure, and ∇n_{dj} is the density gradient of the dust species exist in the negative x direction. For the unperturbed density distribution we assume

$$n_{odj}(x) = n_{odj} e^{-\lambda x} \quad (2.3)$$

where λ is in-homogeneity scale length, Consider zero order state, in which

$$\mathbf{v}_{odjx} = 0, \quad \mathbf{v}_{odjy} = \text{constant}, \quad \mathbf{v}_{odjz} = \mathbf{v}_{odjz}(x) \quad (2.4)$$

$$\nabla\phi_o = \left(\frac{\partial\phi_o}{\partial x} \right) \hat{x}, \quad \text{and} \quad \left(\frac{\partial\phi_o}{\partial y} = 0 = \frac{\partial\phi_o}{\partial z} \right) \quad (2.5)$$

Obviously we included $\left(\frac{\partial\phi_o}{\partial z} = 0 \right)$ in the absence of electric field. For equilibrium state, the equation of motion and continuity will be given as

$$m_{dj} n_{odj} \left(\frac{d \mathbf{v}_{odj}}{dt} + (\mathbf{v}_{odj} \cdot \nabla) \mathbf{v}_{odj} \right) = q_{dj} n_{odj} (\mathbf{E} + \mathbf{v}_{odj} \times \mathbf{B}) - \nabla P \quad (2.6)$$

$$\frac{\partial n_{odj}}{\partial t} + \nabla \cdot (n_{odj} \mathbf{v}_{odj}) = 0 \quad (2.7)$$

By putting the value from Eq.(2.4) and Eq.(2.5), in Eq.(2.6) we have

$$-\lambda \mathbf{V}_{thd}^2 + \frac{q_{dj}}{m_{dj}} \left(\frac{\partial\phi_o}{\partial x} \right) - \omega_{odj} \mathbf{v}_{odjy} = 0 \quad (2.8)$$

where $V_{thd} = \sqrt{\frac{K_B T_{d_j}}{m_{d_j}}}$ is the dust thermal velocity. $\omega_{cdj} = \frac{Z_{d_j} e B}{m_{d_j}}$ is the dust cyclotron frequency with $q_{d_j} = Z_{d_j} e$. Z_{d_j} is the number of charges residing on dust grains and $\lambda = \frac{\nabla n_{odj}(x)}{n_{odj}}$. The density, velocity and potential in perturbed state with time variation can be written respectively as

$$\begin{aligned} n_{1d_j} &= n_{1d_j}(x, y, z) \exp -i\omega t \\ \mathbf{v}_{1d_j} &= \mathbf{v}_{1d_j}(x, y, z) \exp -i\omega t \\ \phi_1 &= \phi_1(x, y, z) \exp -i\omega t \end{aligned} \quad (2.9)$$

Consider waves are propagating along y and z - axis i.e.

$$\vec{k} = (k_y \hat{y} + k_z \hat{z})$$

Then the amplitude of the physical perturbed variables in Eq.(2.9) as the function of space and can be written as

$$\begin{aligned} \tilde{n}_{1d_j}(x, y, z) &= N_{1d_j}(x) e^{i(k_y y + k_z z)} \\ \mathbf{v}_{1d_j}(x, y, z) &= \mathbf{v}_{1d_j}(x) e^{i(k_y y + k_z z)} \\ \phi_{1d_j}(x, y, z) &= \phi_1(x) e^{i(k_y y + k_z z)} \end{aligned}$$

For the study of K-H instability, the system is electrostatically perturbed and fluid wise considered to be linearized. Linearizing equation of continuity and equation of motion by putting $n_{d_j} = n_{odj} + n_{1d_j}$ and $\mathbf{v}_{d_j} = \mathbf{v}_{odj} + \mathbf{v}_{1d_j}$, then applying Fourier transformation i.e. ($\nabla = ik$, $\frac{\partial}{\partial t} = -i\omega_j$) they can be given as respectively,

$$-i\omega_j n_{1d_j} + ik \cdot [(n_{odj} \mathbf{v}_{1d_j} + n_{1d_j} \mathbf{v}_{odj})] = 0 \quad (2.10)$$

$$m_{d_j} n_{odj} [(-i\omega_j) \mathbf{v}_{1d_j} + (\mathbf{v}_{1d_j} \cdot ik) \mathbf{v}_{odj} + (\mathbf{v}_{odj} \cdot ik) \mathbf{v}_{1d_j}] + K_B T_{d_j} ik n_{1d_j} + iq_{d_j} (n_{odj} k \phi_1 + n_{1d_j} k \phi_o)$$

$$-q_{dj}(n_{1dj}\mathbf{v}_{odj} + n_{odj}\mathbf{v}_{1dj}) \times \mathbf{B} = 0 \quad (2.11)$$

As the direction of inhomogeneity is along x - axis then we have

$$\frac{1}{n_{odj}} \frac{\partial N_{1dj}}{\partial x} = \frac{\partial}{\partial x} \left(\frac{N_{1dj}}{n_{odj}} \right) - \lambda \left(\frac{N_{1dj}}{n_{odj}} \right) \quad (2.12)$$

Let for dust species $n_{1dj} = N_{1dj}$ using in Eq.(2.10),

$$-i\omega_j n_{1dj} + ik \cdot (n_{odj}\mathbf{v}_{1dj} + n_{1dj}\mathbf{v}_{odj}) = 0 \quad (2.13)$$

where $ik = \nabla \Rightarrow$

$$-i\omega_j N_{1dj} + \mathbf{v}_{1dj} \cdot \nabla n_{odj} + n_{odj} \nabla \cdot \mathbf{v}_{1dj} + \mathbf{v}_{odj} \cdot \nabla n_{1dj} = 0$$

\Rightarrow

$$-i\omega_j N_{1dj} + \mathbf{v}_{1xdj}(-\lambda n_{odj}) + n_{odj} \left(\frac{\partial \mathbf{v}_{1xdj}}{\partial x} + \frac{\partial \mathbf{v}_{1ydj}}{\partial y} + \frac{\partial \mathbf{v}_{1zdj}}{\partial z} \right) + \frac{\partial N_{1dj}}{\partial y} \mathbf{v}_{oydj} + \frac{\partial N_{1dj}}{\partial z} \mathbf{v}_{ozdj} = 0$$

\Rightarrow

$$\frac{-i\omega_j N_{1dj}}{n_{odj}} - \lambda \mathbf{v}_{1xdj} + \frac{\partial \mathbf{v}_{1xdj}}{\partial x} + ik_y \mathbf{v}_{1ydj} + ik_z \mathbf{v}_{1zdj} + ik_y \frac{N_{1dj}}{n_{odj}} \mathbf{v}_{oydj} + ik_z \frac{N_{1dj}}{n_{odj}} \mathbf{v}_{ozdj} = 0$$

Suppose $\left(\frac{N_{1dj}}{n_{odj}} = \nu_j \right)$ using this notation then above equation will be given as

$$-\lambda \mathbf{v}_{1xdj} + \frac{\partial \mathbf{v}_{1xdj}}{\partial x} + ik_y \mathbf{v}_{1ydj} + ik_z \mathbf{v}_{1zdj} - i(\omega_j - k_y \mathbf{v}_{oydj} - k_z \mathbf{v}_{ozdj}) \nu_j = 0$$

\Rightarrow

$$-\lambda \mathbf{v}_{1xdj} + \left(\frac{\partial \mathbf{v}_{1xdj}}{\partial x} \right) + ik_y \mathbf{v}_{1ydj} + ik_z \mathbf{v}_{1zdj} - i\Omega_j \nu_j = 0 \quad (2.14)$$

where $\Omega_j = \omega_j - k_y \mathbf{v}_{oydj} - k_z \mathbf{v}_{ozdj}$ is the Doppler-shifted frequency with \mathbf{v}_{oydj} and \mathbf{V}_{ozdj} are the streaming velocities along y and z -axis respectively. Similar treatment we have use for Eq.(2.11), for splitting this equation into its x, y and z - components. For this purpose we use Eq.(2.12) and Eq.(2.8). From Eq.(2.8) we use $\frac{q_{dj}}{m_{dj}} \left(\frac{\partial \phi_p}{\partial x} \right) = \omega_{cdj} \mathbf{v}_{oydj} + \lambda \mathbf{V}_{thd}^2$. The x, y and z - components of Eq.(2.11) are given as respectively,

$$\begin{aligned} -i\Omega_j \mathbf{v}_{1xdj} - \omega_{cdj} \mathbf{v}_{1ydj} + \mathbf{V}_{thd}^2 \left(\frac{\partial \nu_j}{\partial x} \right) + \frac{q_{dj}}{m_{dj}} \left(\frac{\partial \phi_1}{\partial x} \right) &= 0 \\ -i\Omega_j \mathbf{v}_{1ydj} + ik_y \mathbf{V}_{thd}^2 \nu_j + \omega_{cdj} \mathbf{v}_{1xdj} + ik_y \left(\frac{q_{dj}}{m_{dj}} \right) \phi_1 &= 0 \\ -i\Omega_j \mathbf{v}_{1zdj} + \mathbf{V}_{thd}^2 ik_z \nu_j + \mathbf{v}_{1zdj} \left(\frac{\partial \mathbf{v}_{ozdj}}{\partial x} \right) + ik_z \left(\frac{q_{dj}}{m_{dj}} \right) \phi_1 &= 0 \end{aligned} \quad (2.15)$$

The set of equations are closed with perturbed neutrality condition with assumption of long wavelength approximation. We have

$$Z_{dj} n_{dj} + n_e = n_i$$

For perturbations the above equation becomes

$$Z_{dj} n_{1dj} + n_{e1} = n_{i1}$$

Above equation called the perturb neutrality condition, by putting $n_{1dj} = N_{1dj}$

\Rightarrow

$$Z_{dj} \frac{N_{1dj}}{n_{odj}} = \frac{n_{e1}}{n_{odj}} - \frac{n_{i1}}{n_{odj}} \quad (2.16)$$

The electrons are assumed to be superthermal (*Non - Maxwellians*), while ions are Boltzmanian. Electrons follow the Kappa distribution function. The kappa distribution function is given as

$$f(r, v) = \frac{n}{2\pi(\kappa\omega_\kappa^2)^{\frac{3}{2}} \Gamma(\kappa - \frac{1}{2}) \Gamma(\frac{3}{2})} \left(1 + \frac{v^2}{\kappa\omega_\kappa^2} \right)^{-(\kappa+1)}$$

Where $\omega_\kappa = \sqrt{\frac{(2\kappa-1)\kappa T}{\kappa m}}$, m, n and T are the thermal velocity, mass, number density

and temperature of the particles. The integration of all velocity space gives number density i.e. $\int_{-\infty}^{+\infty} f(r, v) d^3v = n$ i.e. [132],

$$n_e = n_{e0} \left[1 - \frac{e\phi}{(\kappa - \frac{3}{2})K_B T_e} \right]^{-\kappa + \frac{1}{2}} \quad (2.17)$$

In linearized form with assumption $\frac{e\phi}{K_B T_e} < 1$ we have,

$$n_{e1} = \theta \frac{n_{e0} e\phi}{K_B T_e} \quad (2.18)$$

where $\theta = \left(\frac{\kappa - \frac{1}{2}}{\kappa - \frac{3}{2}} \right)$. Ions are following the Boltzman relation as $n_i = n_{i0} \exp \left[-\frac{e\phi}{K_B T_i} \right]$,

In linearized form we have,

$$n_{i1} = -\frac{n_{i0} e\phi_1}{K_B T_i} \quad (2.19)$$

Putting Eq.(2.18) and (2.19) in Eq.(2.16) with assumption that $\nu_j = \frac{N_{d1}}{n_{d0}}$,

$$\nu_j = \left(\frac{n_{e0}}{Z_{dj} n_{d0j}} \theta + \frac{n_{i0}}{Z_{dj} n_{d0j}} \times \frac{T_e}{T_i} \right) \frac{e\phi_1}{K_B T_e}$$

which implies that

$$\nu_j = \frac{Pe\phi_1}{K_B T_e}$$

where, $P = \theta N_e + N_i \delta$, $N_e = \frac{n_{e0}}{Z_{dj} n_{d0j}}$, $N_i = \frac{n_{i0}}{Z_{dj} n_{d0j}}$ and $\delta = \frac{T_e}{T_i}$. By further simplification above equation will get the following form,

$$\nu_j = \frac{N_{d1}}{n_{d0j}} = \frac{1}{c_{dmj}^2} \frac{e}{m_{dj}} \phi_1 \quad (2.20)$$

where $c_{dmj} = \sqrt{\frac{K_B T_e}{P m_{dj}}}$ is the modified dust acoustic speed. From Eq.(2.15) we get x , y and z component of velocities which are given as,

$$\begin{aligned}
\mathbf{v}_{1xdj} &= \left(\frac{-ik_y}{B(1-\xi_j^2)} \right) \left[1 + \frac{\mathbf{V}_{thd}^2}{c_{dmj}^2} \right] \phi_1 \\
\mathbf{v}_{1y dj} &= \left(\frac{-k_y \xi_j}{B(1-\xi_j^2)} \right) \left[1 + \frac{\mathbf{V}_{thd}^2}{c_{dmj}^2} \right] \phi_1 \\
\mathbf{v}_{1z dj} &= \left(\frac{-ik_z}{B(A-i\xi_j)} \right) \left[1 + \frac{\mathbf{V}_{thd}^2}{c_{dmj}^2} \right] \phi_1
\end{aligned} \tag{2.21}$$

where $\xi_j = \frac{\Omega_j}{\omega_{cdj}}$, $A = \frac{1}{\omega_{cdj}} \left(\frac{\partial V_{cdjz}}{\partial x} \right)$ is dust sheared flow and $\mathbf{V}_{thd} = \sqrt{\frac{k_B T_d}{m_{dj}}}$ is dust thermal speed. These components of velocity show that these are modified by dust sheared flow. By putting the values of \mathbf{v}_{1xdj} , $\mathbf{v}_{1y dj}$ and $\mathbf{v}_{1z dj}$ in Eq.(2.14), we obtain the dispersion relation:

$$\xi_j^4 - \xi_j^2 + i\xi_j^3 A - i\xi_j A - i\beta_j \Lambda_j H_j A + \beta_j \Lambda_j H_j \xi_j - i\xi_j \beta_j^2 H_j - \xi_j^2 \beta_j^2 H_j + \gamma_j^2 H_j - \gamma_j^2 \xi_j^2 H_j = 0, \tag{2.22}$$

where $H_j = (1 + \frac{\mathbf{V}_{thd}^2}{c_{dmj}^2})$, $\beta_j = k_y \rho_j$, where $\rho_j = \frac{c_{dmj}}{\omega_{cdj}}$, is the Larmor radius, $\Lambda_j = \lambda \rho_j$ and $\gamma_j = k_z \rho_j$. For the case of low frequency then ξ_j^4 and $\xi_j^3 \rightarrow 0$, the Eq.(2.22) reduce in to

$$\xi_j^2 + \xi_j (iA - \beta_j \Lambda_j H_j) - i\beta_j \Lambda_j H_j A = 0 \tag{2.23}$$

Let $\xi_j = \omega_j - \omega_{dij}$, where ω_j and $\omega_{dij} = \omega_{yij} + \omega_{zj}$ are the normalized mode frequency and Doppler frequency respectively. These frequencies are normalized with dust cyclotron frequency ω_{cdj} . By using value of ξ_j in Eq.(2.23) we will get,

$$\omega_j^2 + \omega_{yij}^2 - 2\omega_j \omega_{yij} + iA\omega_j - \beta_j \Lambda_j H_j \omega_j - iA\omega_{yij} + \omega_{yij} \beta_j \Lambda_j H_j - iA\beta_j \Lambda_j H_j = 0 \tag{2.24}$$

Eq.(2.24) is a generalized dispersion relation in terms of ω . This equation has complex nature as some source terms responsible for instability in the system are involved like density inhomogeneity and sheared flow. In order to discuss the instability process (KH-instability), let $\omega_j = \omega_{rj} + i\Gamma_j$, where ω_{rj} and Γ_j are the real frequency and growth

rate of KH-mode respectively. By using this value of ω in Eq.2.24 we obtained,

$$\begin{aligned} \omega_{rj}^2 - \Gamma_j^2 + 2i\omega_{rj}\Gamma_j + \omega_{yzj}^2 - 2\omega_{yzj}(\omega_{rj} + i\Gamma_j) + iA(\omega_{rj} + i\Gamma_j) - \beta_j\Lambda_j H_j(\omega_{rj} + i\Gamma_j) - iA\omega_{yzj} \\ + \omega_{yzj}(\beta_j\Lambda_j H_j) - i\beta_j\Lambda_j H_j A = 0 \end{aligned} \quad (2.25)$$

splitting the real and imaginary parts of Eq.2.25 the real part is,

$$\omega_{rj}^2 - \Gamma_j^2 + \omega_{yzj}^2 - 2\omega_{yzj}\omega_{rj} - A\Gamma_j - \beta_j\Lambda_j H_j\omega_{rj} + \omega_{yzj}(\beta_j\Lambda_j H_j) = 0$$

while imaginary part is

$$2\omega_{rj}\Gamma_j - 2\omega_{yzj}\Gamma_j + A\omega_{rj} + \beta_j\Lambda_j H_j\Gamma_j - A\omega_{yzj} - \beta_j\Lambda_j H_j A = 0$$

Simplifying imaginary part, we get the growth rate as

$$\Gamma_j = \left(\frac{T_{Oj} - A\omega_{rj(1,2)}}{2\omega_{rj(1,2)} - D_{Oj}} \right) \quad (2.26)$$

Here $T_{Oj} = A\omega_{yzj} + \beta_j\Lambda_j H_j A$, and $D_{Oj} = 2\omega_{yzj} + \beta_j\Lambda_j H_j$. For positive dust species the growth rate will be

$$\Gamma_+ = \left(\frac{T_{O+} - A\omega_{r+(1,2)}}{2\omega_{r+(1,2)} - D_{O+}} \right) \quad (2.27)$$

While for negative dust

$$\Gamma_- = \left(\frac{T_{O-} - A\omega_{r-(1,2)}}{2\omega_{r-(1,2)} - D_{O-}} \right) \quad (2.28)$$

Using this value of Γ_j in real part, we get the real frequency

$$\omega_{rj}^2 - \left(\frac{T_{Oj} - A\omega_{rj(1,2)}}{2\omega_{rj(1,2)} - D_{Oj}} \right)^2 - D_{Oj}\omega_{rj} - A \left(\frac{T_{Oj} - A\omega_{rj(1,2)}}{2\omega_{rj(1,2)} - D_{Oj}} \right) + Q_{Oj} = 0$$

where $Q_{Oj} = \omega_{yzj}^2 + \omega_{yzj}(\beta_j\Lambda_j H_j)$. By simplification above equation reduces into

quadratic form which is given as,

$$\omega_{rj(1,2)}^2 \Psi_j - \omega_{rj(1,2)} \eta_j - \chi_j = 0$$

Its solution is

$$\omega_{rj(1,2)} = \frac{\eta_j \pm \sqrt{\eta_j^2 + 4\Psi_j\chi_j}}{2\Psi_j} \quad (2.29)$$

For positive dust particles

$$\omega_{r+(1,2)} = \frac{\eta_+ \pm \sqrt{\eta_+^2 + 4\Psi_+\chi_+}}{2\Psi_+} \quad (2.30)$$

For negative dust particles

$$\omega_{r-(1,2)} = \frac{\eta_- \pm \sqrt{\eta_-^2 + 4\Psi_-\chi_-}}{2\Psi_-} \quad (2.31)$$

where, again

$$\begin{aligned} \Psi_j &= 5(2\omega_{yzj} + \beta_j \Lambda_j H_j)^2 + A^2 + 4(\omega_{yzj}^2 + \omega_{yzj} \beta_j \Lambda_j H_j) \\ \eta_j &= (2\omega_{yzj} + \beta_j \Lambda_j H_j)^3 + A^2(2\omega_{yzj} + \beta_j \Lambda_j H_j) + 4(2\omega_{yzj} + \beta_j \Lambda_j H_j)(\omega_{yzj} + \omega_{yzj} \beta_j \Lambda_j H_j) \\ \chi_j &= (A\omega_{yzj} + A\beta_j \Lambda_j H_j)(2\omega_{yzj} + \beta_j \Lambda_j H_j) - A^2(\omega_{yzj} + \beta_j \Lambda_j H_j)^2 + \\ &\quad (2\omega_{yzj} + \beta_j \Lambda_j H_j)^2(\omega_{yzj}^2 + \omega_{yzj} \beta_j \Lambda_j H_j) \end{aligned}$$

All these are constant terms, depends on different physical parameters, like number density, sheared flow and polarity of dust particles.

2.3 Results and discussions

In this section we will discuss the numerical analysis of electrostatic KH-mode in dusty plasma with *Kappa* distributed electrons. The numerical results are plotted for both real frequency and (two and 3-dimensional views) and growth rates as derived mathe-

matically in Equations (2.26) and (2.29) for positive and negative dust particles. We used the following Saturns rings data in *CGS* system [133], where

$$\begin{aligned}
\mathbf{B} &= 0.0004 \rightarrow 0.0006 \text{ gauss} \\
T_e &= 1.15 \times 10^4 \rightarrow 1.15 \times 10^6 \text{ K} \\
T_i &= 1.15 \times 10^3 \text{ K} \\
T_d &= 1.15 \times 10^2 \text{ K} \\
\kappa &= 2 \rightarrow 5 \\
A &= 0.01 \rightarrow 0.03 \\
K_B &= 1.38 \times 10^{-16} \text{ erg/deg(K)} \\
e &= 4.79686 \times 10^{-10} \text{ statcoulomb} \\
Z_{d+} &= 10 \\
Z_{d-} &= 100 \\
m_{d+} &= 4 \times 10^{-12} \text{ g} \\
m_{d-} &= 3.01 \times 10^{-12} \text{ g} \\
n_{i0} &= 28/\text{cm}^3 \\
n_{dj0} &= 10^{-1} - 10^{-2}/\text{cm}^3 \\
n_{e0} &= 29/\text{cm}^3
\end{aligned}$$

Similarly arbitrary values of

$$\begin{aligned}
k_y &= 5k_x \\
\mathbf{v}_{\alpha y dj} &= 0.01 c_{dmj} \\
\mathbf{v}_{\alpha z dj} &= 0.02 c_{dmj}
\end{aligned}$$

2.3.1 KH- instability with positive dust polarity

The effect of Kappa index in the dusty plasma on the real frequency of KH mode, using Eq.(2.30) is shown in Fig 2.1 (a) and (b). Fig 2.1 (a) shows the 2-dimensional

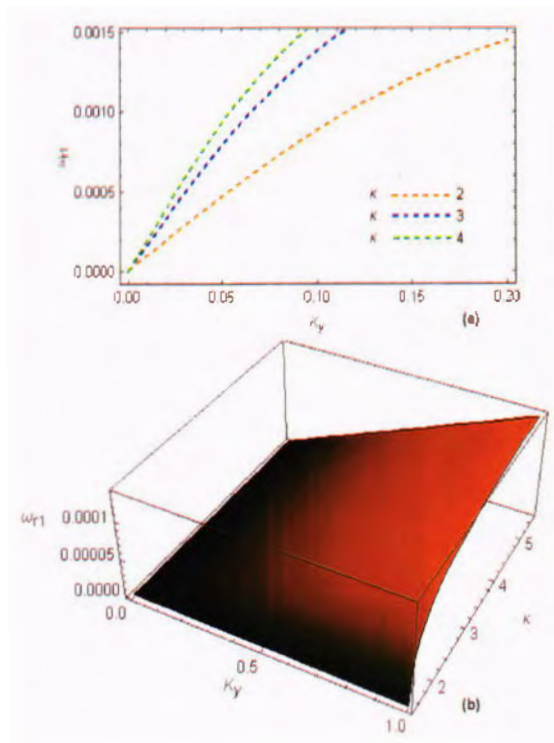


Figure 2.1: The graphical representation of normalized frequency ω_{r1} of KH modes. (a) as a function of K_y for different values of $\kappa = 2$ (red dotted line), $\kappa = 3$ (blue dotted line) and $\kappa = 4$ (green dotted line), while (b) is the 3-dimensional view with k_y and κ . All others parameters are taken arbitrary from section of result and discussion.

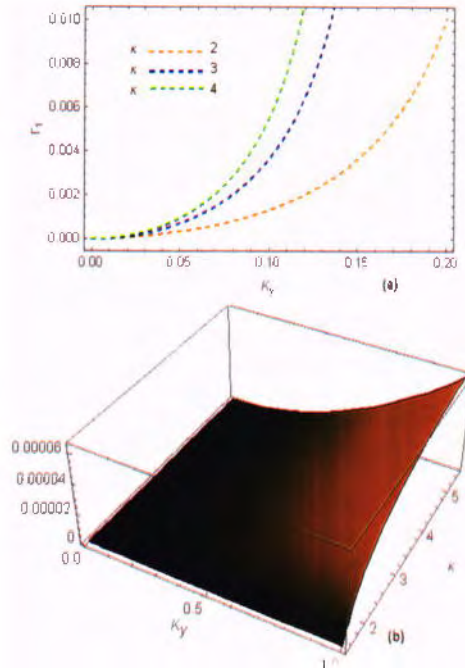


Figure 2.2: The graphical representation of growth rate Γ_1 of KH modes. (a) as a function of k_y for different values of $\kappa = 2$ (red dotted line), $\kappa = 3$ (blue dotted line) and $\kappa = 4$ (green dotted line) and (b) is the 3-dimensional view with k_y and κ .

variation of real part of frequency versus wave number of KH-instability, with the effect of different values of κ such that $\kappa = 2$ (red dotted line), $\kappa = 3$ (blue dotted line) and $\kappa = 4$ (dotted green line). The corresponding 3-D view is shown in Fig. 2.1 (b). These figures show that the real frequency increases by increasing the values of κ . It means that for positive dust particles when a system is approaching towards Maxwellian, its phase speed increases. It further means that KH-mode gains energy when the system is approaching towards Maxwellian.

Fig 2.2(a) and (b) shows the variation of growth rate of Eq. (2.27) versus wave number of KH-instability in dusty plasma with the effect kappa index κ , such that $\kappa = 2$ (red dotted line), $\kappa = 3$ (blue dotted line) and $\kappa = 4$ (green dotted line). Fig. 2.2(b) shows the 3 - D representation of the growth rate with respect to k_y and κ . These show that the growth rate of KH instability increases with increasing values of κ . It means that the greater value of κ makes the system unstable, for positive dust particles.

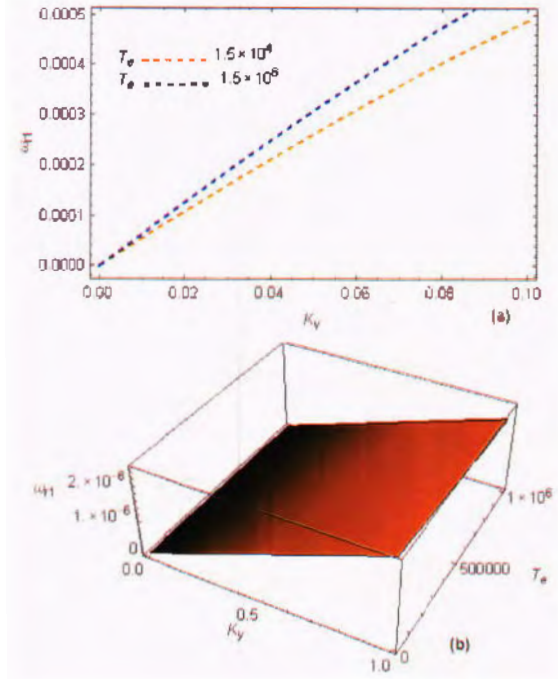


Figure 2.3: (a) Variation of real frequency ω_{r1} as a function of k_y , for different values of electron temperature such that $T_e = 1.15 \times 10^4$ (red dotted) line and for $T_e = 1.15 \times 10^6$ (blue dotted line), while (b) is the 3-D representation of frequency with effect of temperature of electron.

Fig. 2.3(a) shows the variation of real frequency as a function of wave vector of KH instability for different values of temperature of electrons such that $T_e = 1.15 \times 10^4$ (red dotted line) and for $T_e = 1.16 \times 10^6$ (blue dotted line). Fig. 2.3(b) shows the 3-D view of the real frequency of KH-instability with respect to k_y and T_e . These figures show that the real frequency of KH instability increases with increasing the temperature of electron. Enhancing temperature means that more energetic electrons and with mode interaction these electrons impart energy to the mode, consequently enhances its phase-speed. Enhancing phase speed causes the mode dispersive and non-linear.

Fig. 2.4(a) shows the variation of growth rate as a function of wave vector k_y of KH instability for different values of temperature of electron such that $T_e = 1.15 \times 10^4$ (red dotted line) and $T_e = 1.16 \times 10^6$ (blue dotted line) with 3-D views in 2nd part of the figure. It shows that the growth rate of KH instability increases with increasing the value of temperature of electron. Increasing temperature of electrons means enhancing thermal energy of electrons. These energetic electrons make system unstable.

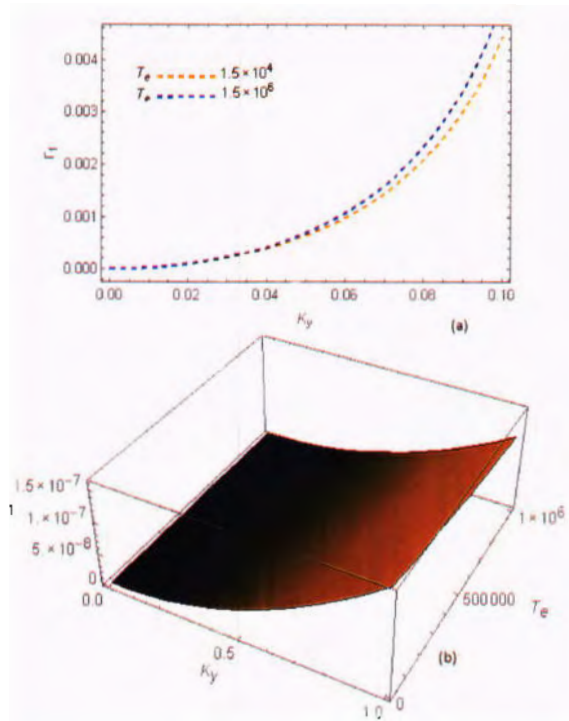


Figure 2.4: (a) Variation of real frequency Γ_1 as a function of k_y , for different values of electron temperature such that $T_e = 1.15 \times 10^4$ (red dotted) line and for $T_e = 1.15 \times 10^6$ (blue dotted line), while (b) is the 3-D representation of frequency with effect of temperature of electron.

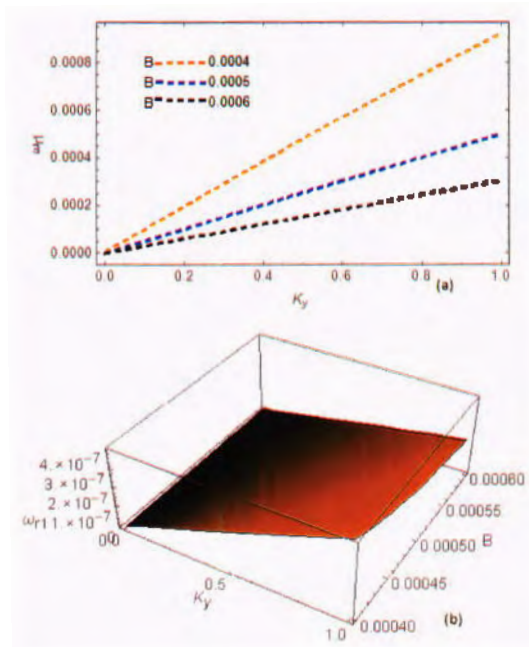


Figure 2.5: (a) Variation of real frequency ω_{r1} as a function of wave vector k_y , for different values of magnetic field such that $B = 0.0004$ (red dotted line), $B = 0.0005$ (blue dotted line) and $B = 0.0006$ (black dotted line), while (b) is the 3-D representation of frequency with effect of magnetic field. The physical parameters are taken from the section of result and discussions.

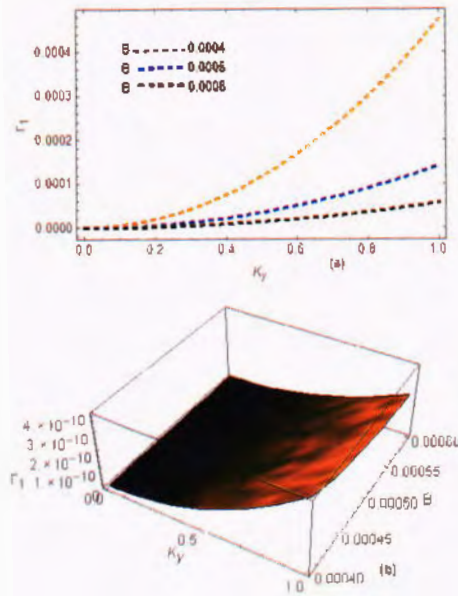


Figure 2.6: (a) Variation of growth rate Γ_1 as a function of wave vector k_y , for different values of magnetic field such that $B = 0.0004$ (red dotted line), $B = 0.0005$ (blue dotted line) and $B = 0.0006$ (black dotted line), while (b) is the 3-D representation of growth rate with effect of magnetic field.

The variation of real frequency as a function of k_y , with different values of B is shown in Fig. 2.5, where (a) is the 2-dimensional and (b) is the 3-D views of KH-mode variation in dusty plasma with positive polarity. This figure shows that the real frequency of KH instability decreases with increasing values of magnetic field. The corresponding growth rate variation both in 2-D and 3-D with respect to B is shown in Fig. 2.6 (a) and (b). This Fig.2.6 also reveals that the growth rate of KH instability decreases with increasing values of magnetic field. Physically this means that the external applied magnetic field have a stabilizing effect on the growth rate of KH-instability. This means particles are more confined to the center, than periphery.

Fig. 2.7(a) show the variation of real frequency of KH instability for different values of shear flow such that $A = 0.01$ (red dotted line), $A = 0.02$ (blue dotted line) and $A = 0.03$ (black dotted line) and the corresponding 3-D plot with respect to A is shown in Fig. 2.7(b). The figure overall shows that the real frequency of KH instability increases with increasing the values of sheared flow. Our wave mode is defined between

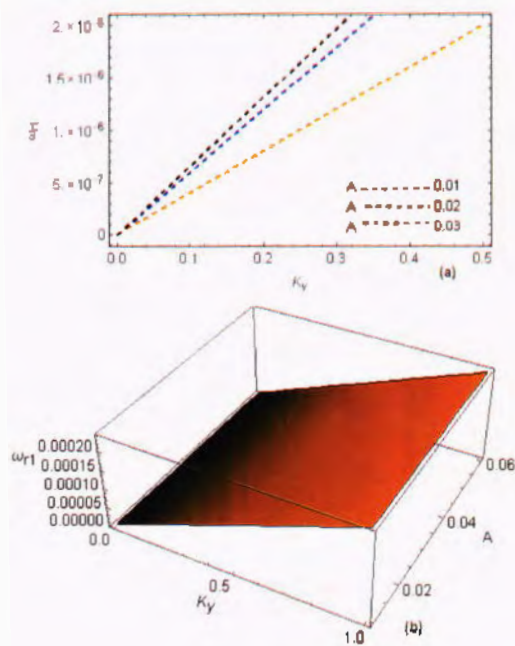


Figure 2.7: (a) Variation of real frequency ω_{r1} as a function of wave vector k_y , for different values of sheared flow such that $A = 0.01$ (red dotted line), $A = 0.02$ (blue dotted line) and $A = 0.03$ (black dotted line), while (b) is the 3-D representation of frequency with effect of sheared flow.

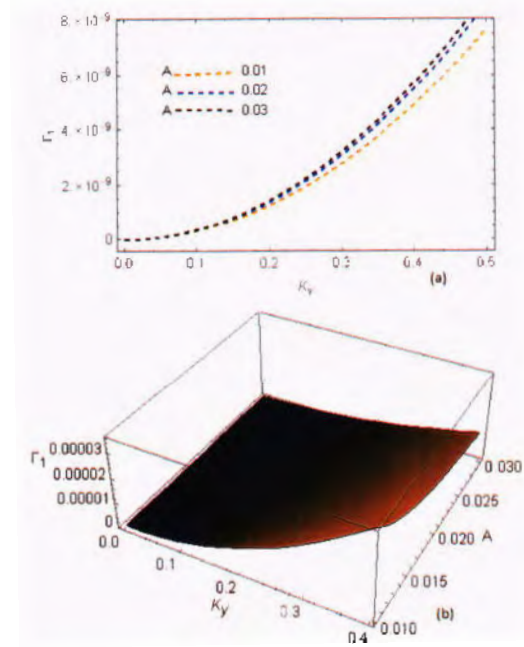


Figure 2.8: (a) Variation of growth rate Γ_1 as a function of wave vector K_y , for different values of sheared flow such that $A = 0.01$ (red dotted line), $A = 0.02$ (blue dotted line) and $A = 0.03$ (black dotted line), while (b) is the 3-D representation of growth rate with effect of sheared flow.

two dimensions i.e. k_y and k_z . Since the sheared flow is along z -axis as a function of x i.e. $\mathbf{v}_{oz\hat{t}j} = \mathbf{v}_{oz\hat{t}j}(\mathbf{x})$. This shear flow enhance the frequency of K-H modes.

Fig. 2.8(a) shows the 2-D variation of growth rate as a function of wave vector of KH mode for different values of sheared flow A such that $A = 0.01$ (red dotted line), $A = 0.02$ (blue dotted line) and $A = 0.03$ (green dotted line) while its 3-D interpretation is shown in 2nd part of the figure. This reveals that the growth rate of KH-instability increases with increasing the values of the positive dust shear flow A . Physically this means that positive dust sheared flow makes the system unstable at its maximum values.

2.3.2 KH-instability analysis with negative dust polarity

The effect of Kappa index in the dusty plasma on the real frequency of KH mode for negative dust particles using Eq.(2.31) is shown in Fig 2.9 (a) and (b). Fig 2.9 (a) shows the 2-dimensional variation of real part of frequency versus wave number

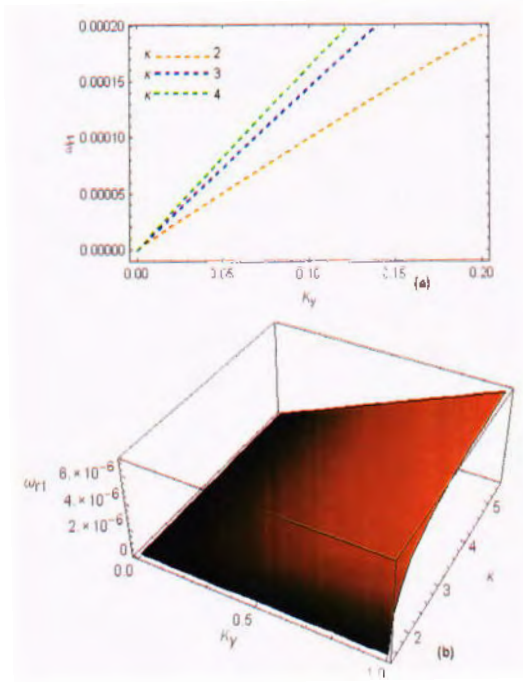


Figure 2.9: The graphical representation of normalized frequency ω_{r1} of KH modes. (a) as a function of k_y for different values of $\kappa = 2$ (red dotted line), $\kappa = 3$ (blue dotted line) and $\kappa = 4$ (green dotted line), while (b) is the 3-dimensional view with k_y and κ .

of KH-instability, with the effect of different values of κ such that $\kappa = 2$ (red dotted line), $\kappa = 3$ (blue dotted line) and $\kappa = 4$ (green dotted line). The corresponding 3-D view is shown in Fig. 2.9 (b). These figures show that the real frequency increases by increasing the values of κ . It means that for negative dust particles when a system is approaching towards Maxwellian, its phase speed increases. It further means that KH-mode gains energy when the system is approaching towards Maxwellian. In both positive and negative case, the frequency of KH-mode increases, but the trend of mode frequency, and magnitude of variation is quite different.

Fig 2.10 (a) and (b) shows the variation of growth rate Eq. (2.28) versus wave number of KH-instability in dusty plasma with the effect kappa index κ , such that $\kappa = 2$ (red dotted line), $\kappa = 3$ (blue dotted line) and $\kappa = 4$ (green dotted line). Fig. 2.10 (b) shows the 3-D representation of the growth rate with respect to k_y and κ . This reveals that the growth rate of KH instability decreases with increasing values of κ . It means that the greater value of κ makes the system stable. The system goes towards Maxwellian, when we increase value of κ . Hence for increasing the value of κ

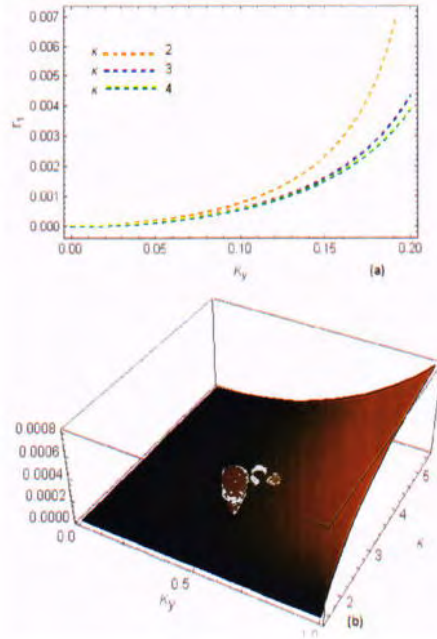


Figure 2.10: The graphical representation of normalized frequency ω_{r1} of KH modes. (a) as a function of k_y for different values of $\kappa = 2$ (red dotted line), $\kappa = 3$ (blue dotted line) and $\kappa = 4$ (green dotted line), while (b) is the 3-dimensional view with k_y and κ .

K-H modes become stable for the case of negative dust species.

Fig. 2.11 (a) shows the variation of real frequency as a function of wave vector of KH instability for different values of temperature of electrons such that $T_e = 1.15 \times 10^4$ (red dotted line) and for $T_e = 1.16 \times 10^6$ (blue dotted line). Fig. 2.11 (b) shows the 3-D view of the real frequency of KH-instability with respect to k_y and T_e . These show that the real frequency of KH instability decreases with increasing the temperature of electron. Enhancing temperature means that more energetic electrons, consequently decreases the phase-speed, for negative dust species.

Fig. 2.12 (a) shows the variation of growth rate as a function of wave vector of KH instability for different values of temperature of electron such that $T_e = 1.15 \times 10^4$ (red dotted line) and $T_e = 1.16 \times 10^6$ (blue dotted line) with 3-D views in 2nd part of the figure. It shows that the growth rate of KH instability decreases with increasing the value of temperature of electron. This reveals that for negative dust particles due to thermal electrons system is going towards stable conditions. These higher energetic electrons have stabilizing effect.

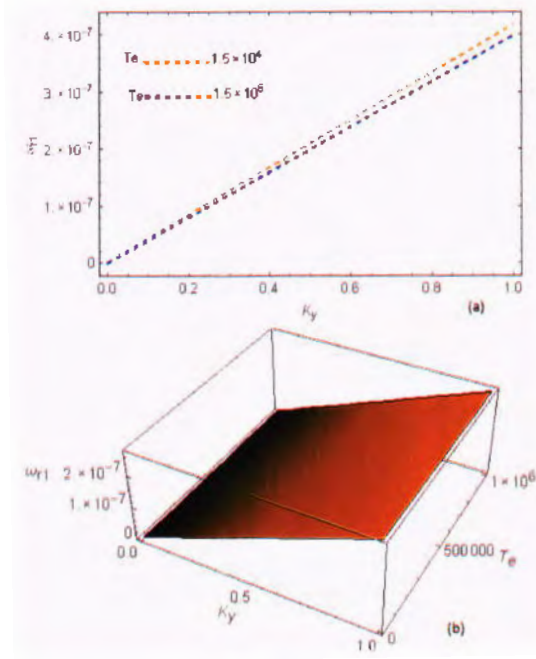


Figure 2.11: (a) Variation of real frequency ω_{r1} as a function of k_y , for different values of electron temperature such that $T_e = 1.15 \times 10^4$ (red dotted) line and for $T_e = 1.15 \times 10^8$ (blue dotted line), while (b) is the 3-D representation of frequency with effect of temperature of electron.

Fig. 2.13 (a) shows the variation of real frequency versus wave vector of KH mode for different values of magnetic field such that $B = 0.0004$ (red dotted line), $B = 0.0005$ (blue dotted line) and for $B = 0.0006$ (black dotted line). It shows that the real frequency of KH instability decreases with increasing the value of magnetic field. The corresponding growth rate variation both in 2-D and 3-D with respect to B is shown in Fig. 2.14 (a) and (b). This Fig.2.14 also reveals that the growth rate of KH instability increases with increasing values of magnetic field. Physically this means that the external applied magnetic field have a destabilizing effect on the growth rate of KH-instability.

Fig. 2.15 (a) show the variation of real frequency of KH instability for different values of shear flow such that $A = 0.01$ (red dotted line), $A = 0.02$ (blue dotted line) and $A = 0.03$ (black dotted line) and the corresponding 3-D plot with respect to A is shown in Fig. 2.14 (b). The figure overall shows that the real frequency of KH instability increases with increasing the values of sheared flow. Thus the sheared flow

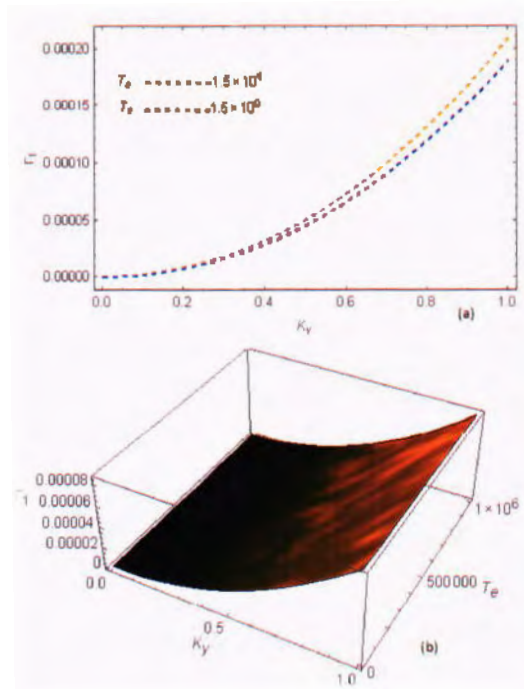


Figure 2.12: (a) Variation of real frequency Γ_1 as a function of k_y , for different values of electron temperature such that $T_e = 1.15 \times 10^4$ (red dotted) line and for $T_e = 1.15 \times 10^6$ (blue dotted line), while (b) is the 3-D representation of frequency with effect of temperature of electron.

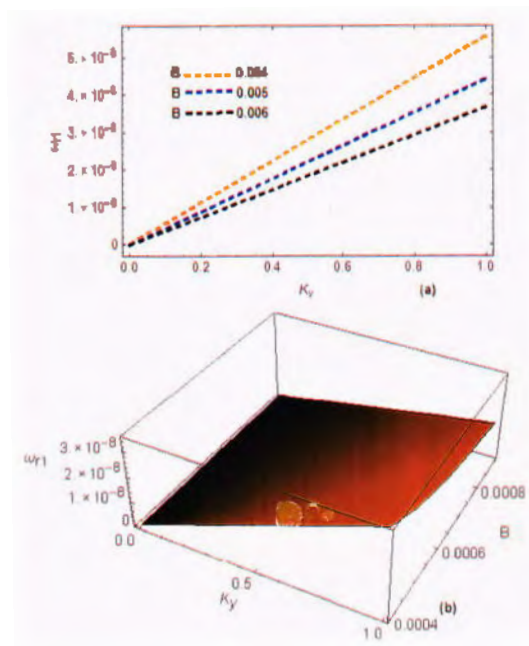


Figure 2.13: (a) Variation of real frequency ω_{r1} as a function of wave vector k_y , for different values of magnetic field such that $B = 0.0004$ (red dotted line), $B = 0.0005$ (blue dotted line) and $B = 0.0006$ (black dotted line), while (b) is the 3-D representation of frequency with effect of magnetic field. The physical parameters are taken from the section of result and discussion.

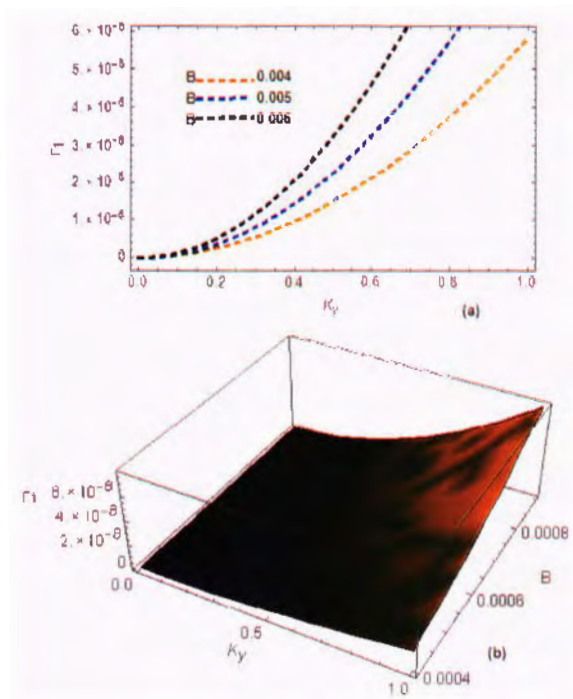


Figure 2.14: (a) Variation of growth rate Γ_1 as a function of wave vector K_y , for different values of magnetic field such that $B = 0.0004$ (red dotted line), $B = 0.0005$ (blue dotted line) and $B = 0.0006$ (black dotted line), while (b) is the 3-D representation of growth rate with effect of magnetic field.

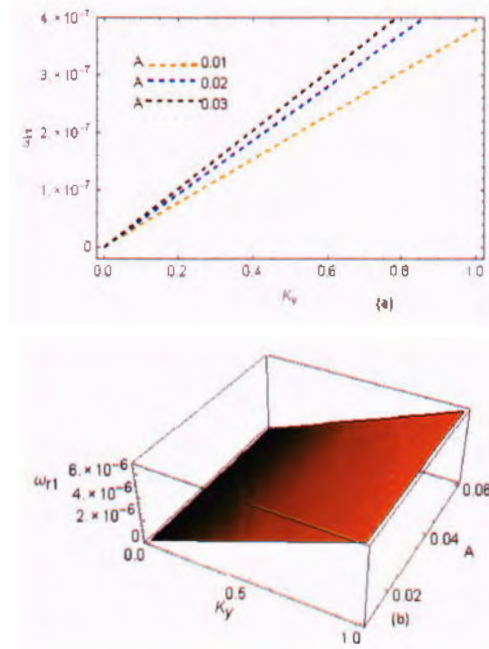


Figure 2.15: (a) Variation of real frequency ω_{r1} as a function of wave vector k_y , for different values of sheared flow such that $A = 0.01$ (red dotted line), $A = 0.02$ (blue dotted line) and $A = 0.03$ (black dotted line), while (b) is the 3-D representation of frequency with effect of sheared flow.

cause by negative dust species enhances phase speed.

Fig. 2.16 (a) shows the 2-D variation of growth rate as a function of wave vector of KH mode for different values of sheared flow A such that $A = 0.01$ (red dotted line), $A = 0.02$ (blue dotted line) and $A = 0.03$ (green dotted line) while its 3-D interpretation is shown in 2nd part of the figure. This reveals that the growth rate of KH-instability decreases with increasing the values of the negative dust shear flow A . Physically this means that negative dust sheared flow makes the system stable at maximum values of A .

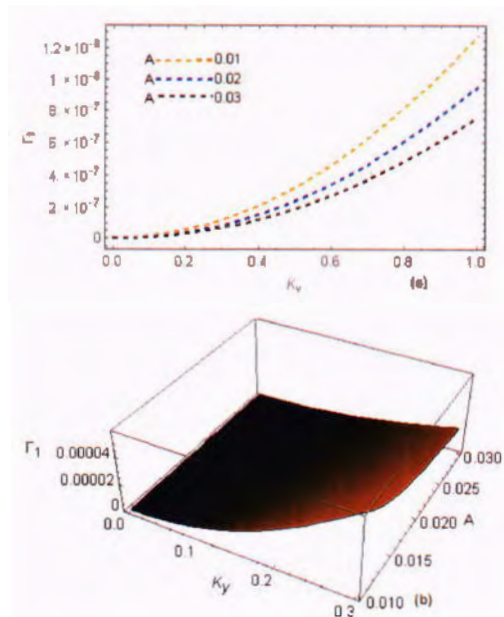


Figure 2.16: (a) Variation of growth rate Γ_1 as a function of wave vector k_y , for different values of sheared flow such that $A = 0.01$ (red dotted line), $A = 0.02$ (blue dotted line) and $A = 0.03$ (black dotted line), while (b) is the 3-D representation of growth rate with effect of sheared flow.

Chapter 3

Summary and Conclusions

In this thesis, we have studied the effect of superthermal (Kappa distributed) electrons on Kelvin-Helmholtz instability in four component dusty plasma. Our main focus was on the investigation of polarity effect on KH modes. For this purpose, we have used the hydrodynamic equations for low beta β plasma with the assumption that ions are Maxwellian while electrons follow non-Maxwellian distribution i.e. (*Kappa distribution*). A generalized dispersion relation for KH instability has been obtained analytically and numerically as well. By solving quadratic equation we face real and imaginary parts, where from real part of wave gives the dispersion relation while imaginary part embodies the growth rate of K-H modes. The two relations of real frequency have been obtained i.e. ω_{r1} and ω_{r2} . The ω_{r1} is for forward modes while ω_{r2} represents back coming modes. For the case of positive and negative dust particles we have checked the polarity effect on the K-H modes by changing the values of different parameters such as kappa index κ electrons temperature T_e , magnetic field B and dust sheared flow A .

o By increasing value of kappa index κ from 2 \rightarrow 4 we observed that the for positive dust species the real frequency and growth rate are increasing. This reveals to us that the system is unstable. But for the negative dust species we observed that the real frequency is increasing while growth rate is decreasing. Hence the system is going towards Maxwellian, by increasing the value of kappa index κ , and it has stabilizing effect on system for negative dust species.

◦ For the case of positive dust by increasing the value of electron temperature T_e from 1.15×10^4 to 1.15×10^6 both the real frequency and growth rate were observed increasing. As the electrons are considered superthermal following kappa distribution then our system is going towards unstable conditions i.e. instability occurs. But for the case of negative dust species we observed that the both real frequency and growth are decreasing. This reveals that the our system is going towards stable condition for the negative dust species.

◦ Similarly by changing the value of magnetic field B from 0.0004 \rightarrow 0.0006, the real frequency for both positive and negative dust species is decreasing. The growth rate is decreasing for positive dust species, but increasing for negative dust species, hence magnetic field also has stabilizing and destabilizing effect on our plasma system respectively. This mean that for positive dust species the particles are confined to center, while for negative dust species the particles are at periphery.

◦ We are familiar that in dusty plasma the dust sheared flow is the main player for the cause of K-H instability. By changing value of dust sheared A from 0.01 \rightarrow 0.03, we observed that, for the case of positive dust species the both real frequency and growth rates are increasing. Hence system is going towards the unstable conditions and sheared flow caused by positive dust species increases the K-H modes. While for negative dust species the real frequency increases with increasing the value of A , but growth rate is decreasing. Hence our system is going towards the stabilizing conditions.

Bibliography

- [1] F.F Chen, *Introduction to Plasma physics & Controlled Fusion*, 2nd Edition volume Plenum Press, New York 1983.
- [2] R. D. Nicholson, *Introduction to plasma theory*, Wiley, New York USA, 1983.
- [3] <http://concentratingsolarpowerutility.com/nuclearmhd.jpg>.
- [4] J. A. Bittencourt, *Fundamentals of Plasma Physics*, Pergamon Press, First Edition, 1986.
- [5] Heinlin, Julia, et al. Plasma medicine possible applications in dermatology *Journal der Deutschen Dermatologischen Gesellschaft*, **12** (2010) 968-976.
- [6] M.G. Kong, et al. Plasma medicine an introductory review, *New Journal of Physics*, **11** (2009) 115012 .
- [7] Heinlin, Julia, et al. Plasma medicine possible applications in dermatology *Journal der Deutschen Dermatologischen Gesellschaft*, **12** (2010) 968-976.
- [8] E. P. Liang, S.C.Wilks, and M. Tabak, *Phys Rev Lett*, **81** (1998) 4887.
- [9] N. Iwamoto, *Phys Rev E.*, **47** (1993) 604 .
- [10] A. Mushtaq, and H. A. Shah, Effects of positron concentration ion temperature, and plasma β value on linear and nonlinear two-dimensional magnetosonic waves in electron-positron-ion plasmas, *Physics of plasmas*, **1** (2005) 012301-012301.
- [11] M. J. Rees, *In The Very Early Universe*, Cambridge University Press, Cambridge, 1983.

- [12] S. Weinberg, *Gravitation and Cosmology*, Wiley, New York, 1972.
- [13] R. L. Merlino, Dusty plasmas and applications in space and industry, *Plasma Physics Applied*, **81** (2006) 73-110.
- [14] A. Bouchoule, *Dusty Plasmas Physics Chemistry and Technological Impacts in Plasma Processing*, John Wiley, Chichester 1999.
- [15] P. K. Shukla, *Astrophys Space Sci*, **264** (1999) 235.
- [16] P. M. Bellan, *Fundamental of plasma physics*, Cambridge University Press, New York, 2006.
- [17] M. Rosenberg, *Planet. Space Sci*, **41** (1993) 229.
- [18] M. S. Sodha and S. Guha, *Advances in Plasma Physics*, **4** (1971) 219-309.
- [19] V. W. Chow, D. A. Mendis, and M. Rosenberg, Role of grain size and particle velocity distribution in secondary electron emission in space plasmas, *Journal of Geophysical Research Space Physics*, **98** (1993) 19065-19076.
- [20] E.C. Whipple, Potentials of surfaces in space, *Reports on Progress in Physics*, **44** (1981) 1197.
- [21] V.E. Fortov, et al. Dusty plasmas *Physics-Uspekhi*, **47** (2004) 447-492.
- [22] U. De Angelis, The physics of dusty plasmas *Physica Scripta*, **45** (1992) 465.
- [23] S. Messenger, Identification of molecular-cloud material in interplanetary dust particles, *Nature*, **404** (2000) 968.
- [24] <https://earthandsolarsystem.files.wordpress.com/2011/06/p101.png>.
- [25] B. A. Smith, et al. Encounter with Saturn Voyager 1 imaging science results, *Science*, **212** (1981) 163-191.
- [26] B. A. Smith, et al. A new look at the Saturn system, The Voyager 2 images, *Science*, **215** (1982) 504-537.

- [27] Horanyi, Mihaly, Dust streams from Jupiter and Saturn, *Physics of Plasmas*, **7** (2000) 3847-3850.
- [28] Doyle, R. Laurence, Luke Dones, and N. C. Jeffrey, Radiative transfer modeling of Saturn's outer B ring, *Icarus*, **80** (1989) 104-135.
- [29] http://www.aeqt.com/sites/default/files/a/470556_134792.jpg.
- [30] Cho, Y. N. John , and M. C. Kelley, Polar mesosphere summer radar echoes Observations and current theories, *Reviews of Geophysics*, **31** (1993) 243-265.
- [31] T. W. Backhouse, The luminous cirrus cloud of June and July, *Meteorol. Mag*, **20** (1885) 133-133.
- [32] P. A. Bernhardt , G. Ganguli, M. C. Kelley and W. E. Swartz, *J. Geophys. Res*, **100** (1995) 23811.
- [33] <http://en.es-static.us/upl/2015/06/noctilucent-cloud-aurora-6-8-2015-Canada-Harlan-Thomas1.jpg>.
- [34] Lieberman, A. Michael, and A. J. Lichtenberg. *Principles of plasma discharges and materials processing*, John Wiley & Sons, 2005.
- [35] C. Thompson, et al. Dust acoustic waves in a direct current glow discharge, *Physics of Plasmas*, **4** (1997) 2331-2335.
- [36] Xu, Wenjun, et al. A dusty plasma device for producing extended, steady state, magnetized, dusty plasma columns, *Review of scientific instruments*, **63** (1992) 5266-5269.
- [37] R. M. Roth, et al. Spatial dependence of particle light scattering in an rf silane discharge, *Applied Physics Letters*, **46**(3) (1985) 253-255.
- [38] I. Cabarrocas, Pere Roca, et al. Polymorphous silicon thin films produced in dusty plasmas: application to solar cells *Plasma physics and controlled fusion*, **46** (2004) B235.

- [39] E. Stoffels, et al. MoS₂ nanoparticle formation in a low pressure environment, *Journal of applied physics*, **86** (1999) 3442-3451.
- [40] A. Bouchoule,, *Dusty plasma: physics, chemistry, and technological impacts in plasma processing*, John Wiley & Sons Inc, 1999.
- [41] S. I. Krasheninnikov, et al. On dust dynamics in tokamak edge plasmas, *Physics of Plasmas*, **11** (2004) 3141-3150.
- [42] J. Winter, *Plasma Phys. Control Fusion*, **46** (2004) B583 .
- [43] J. Winter, Dust in fusion devices-experimental evidence, possible sources and consequences, *Plasma physics and controlled fusion*, **40** (1998) 1201.
- [44] F. E. Vladimirov and M. E. Gregor, *Complex and Dusty Plasmas From Laboratory to Space*, CRC Press 2010.
- [45] https://cdn.kastatic.org/googleusercontent/jgi5LNR6fg_SmiYwiXM7i08iT46PEJyHd6R6yFz1
- [46] A. Mushtaq, *Analytical and Theoretical Studies of Low Frequency Non-linear Waves in Multi-Component Plasmas*, HEC Ph.d Thesis, (2006).
- [47] F. B. Rizzato, Weak nonlinear electromagnetic waves and low-frequency magnetic-field generation in electron-positron-ion plasmas, *Journal of plasma physics*, **40** (1988) 289-298.
- [48] A. Mushtaq, and S. A. Khan, Ion acoustic solitary wave with weakly transverse perturbations in quantum electron-positron-ion plasma, *Physics of plasmas*, **14** (2007) 052307.
- [49] T. Tajima, and T. Taniuti, Nonlinear interaction of photons and phonons in electron-positron plasmas, *Physical Review A*, **42** (1990) 3587.
- [50] G. Livadiotis, and D. J. McComas, Understanding kappa distributions: A toolbox for space science and astrophysics, *Space Science Reviews*, **175** (2013) 183-214.

- [51] R. A. Cairns, A. A. Mamun, R. Bingham, R. Bostrom, R. O. Dendy, C. M. C. Nairn, and P. K. Shukla, *Geophys. Res. Lett.* **22**, 2709, doi:10.1029/95GL02781 (1995)
- [52] C. Tsallis, Possible generalization of Boltzmann-Gibbs statistics, *Journal of statistical physics*, **52** (1988) 479-487.
- [53] A. A. Abid, et al. Vasyliunas-Cairns distribution function for space plasma species, *Physics of Plasmas*, **22** (2015) 084507.
- [54] A. A. Abid, et al. Vasyliunas-Cairns distribution function for space plasma species, *Physics of Plasmas*, **22** (2015) 084507.
- [55] A. Mushtaq, and Attaullah Shah, Sheared flow-driven vortices and solitary waves in a non-uniform plasma with negative ions and non-thermal distributed electrons *Journal of Plasma Physics*, **79** (2013) 479-487.
- [56] F. Verheest, and S. R. Pillay, Dust-acoustic solitary structures in plasmas with nonthermal electrons and positive dust, *Nonlinear Processes in Geophysics*, **15** (2008) 551.
- [57] H. Schamel, Electron holes, ion holes and double layers: Electrostatic phase space structures in theory and experiment, *Physics reports*, **140** (1986) 161-191.
- [58] X. Qi, et al. Application of Particle-in-Cell Simulation to the Description of Ion Acoustic Solitary Waves, *IEEE Transactions on Plasma Science*, **43** (2015) 3815-3820.
- [59] B. Sahu, P. Swarup and R. Rajkumar, Solitonic, quasi-periodic and periodic pattern of electron acoustic waves in quantum plasma, *Astrophysics and Space Science*, **341** (2012) 567-572.
- [60] V. Munoz, A nonextensive statistics approach for Langmuir waves in relativistic plasmas, *Nonlinear Processes in Geophysics*, **13** (2006) 237-241.

- [61] R. Silva, J. S. Alcaniz, and J. A. S. Lima, Constraining nonextensive statistics with plasma oscillation data, *Physica A: Statistical Mechanics and its Applications*, **356** (2005) 509-516.
- [62] I. B. Bernstein, Waves in a plasma in a magnetic field, *Physical Review*, **109** (1958) 10.
- [63] A. Mushtaq, and H. A. Shah, Study of non-Maxwellian trapped electrons by using generalized (r, q) distribution function and their effects on the dynamics of ion aconstic solitary wave, *Physics of plasmas* **13**(1) (2006) 012303.
- [64] S. Zaheer, G. Murtaza, and H. A. Shah, Some electrostatic modes based on non-Maxwellian distribution functions, *Physics of Plasmas*, **11** (2004) 2246-2255.
- [65] J. J. Podesta, Spatial Landau damping in plasmas with three-dimensional κ distributions, *Physics of plasmas*, **12** (2005) 052101.
- [66] N. Rubab, G. Murtaza, and A. Mushtaq. "Effect of non-Maxwellian particle trapping and dust grain charging on dust acoustic solitary waves." *Physics of plasmas*, **13** (2006) 112104.
- [67] A. Mushtaq and H. A. Shah. "Study of non-Maxwellian trapped electrons by using generalized (r, q) distribution function and their effects on the dynamics of ion acoustic solitary wave, *Physics of plasmas*, **13**(1) (2006) 012303.
- [68] V. Pierrard, and M. Lazar Kappa distributions: theory and applications in space plasmas *Solar Physics*, **267** (2010) 153-174.
- [69] V. M. Vasyliunas, A survey of low-energy electrons in the evening sector of the magnetosphere with OGO 1 and OGO 3, *Journal of Geophysical Research*, **73** (1968) 2839-2884.
- [70] M. Maksimovic, , P. Viviane and R. Pete, Ulysses electron distributions fitted with Kappa functions, *Geophysical research letters*, **24** (1997) 1151-1154.

- [71] A. J. Steffl, B. Fran , and A. Ian F. Stewart. Cassini UVIS observations of the Io plasma torus: II. Radial variations *Icarus*, **172** (2004) 91-103.
- [72] V. Pierrard and M. Lazar, Kappa distributions: theory and applications in space plasmas, *Solar Physics*, **267** (2010) 153-174.
- [73] Hasegawa, Akira, Kunioki Mima, and Minh Duong-van, Plasma distribution function in a superthermal radiation field, *Physical review letters*, **54** (1985) 2608.
- [74] J. D. Scudder, Why all stars should possess circumstellar temperature inversions, *The Astrophysical Journal*, **398** (1992) 319-349.
- [75] B. D. Shizgal, Suprathermal particle distributions in space physics Kappa distributions and entropy, *Astrophysics and Space Science*, **312** (2007) 227-237.
- [76] V. Pierrard and M. Lazar, Kappa distributions: theory and applications in space plasmas, *Solar Physics*, **267** (2010) 153-174.
- [77] Moore, Luke, and Michael Mendillo, Ionospheric contribution to Saturn's inner plasmasphere, *Journal of Geophysical Research Space Physics*, **110** (2005).
- [78] Qureshi, M. N. S., et al. Solar wind particle distribution function fitted via the generalized kappa distribution function Cluster observations, *AIP Conference Proceedings*, **679** (2003).
- [79] Pandey, Rama Shankar, and R. P. Pandey. Cold plasma injection on VLF wave mode for relativistic magnetoplasma with AC electric field, *Progress In Electromagnetics Research C*(2) (2008) 217-232.
- [80] Livadiotis, G., and D. J. McComas, Understanding kappa distributions A toolbox for space science and astrophysics, *Space Science Reviews*, **175** (2013) 183-214.
- [81] T. Saha et al. *Z. Naturforsch.* **64a** (2009) 370-376.
- [82] N. N. Rao, P. K. Shukla, and M. Yu Yu, Dust-acoustic waves in dusty plasmas, *Planetary and space science*, **38** (1990) 543-546.

- [83] A. Barkan, Robert L. Merlino, and N. D'angelo, Laboratory observation of the dust-acoustic wave mode, *Physics of Plasmas*, **2** (1995) 3563-3565.
- [84] N. N. Rao, P. K. Shukla, and M. Yu Yu, Dust-acoustic waves in dusty plasmas, *Planetary and space science*, **38** (1990) 543-546.
- [85] A. A. Mamun, and P. K. Shukla, Solitary potentials in cometary dusty plasmas, *Geophysical research letters*, **29** (2002).
- [86] A. A. Mamun, and P. K. Shukla, Spherical and cylindrical dust acoustic solitary waves, *Physics Letters A*, **290** (2001) 173-175.
- [87] P. K. Shukla, and A. A. Mamun, *Introduction to Dusty plasma Physics*, Institute of Physics, Bristol, 2002.
- [88] P. K. Shukla, and V. P. Silin, Dust ion-acoustic wave, *Physica Scripta*, **45** (1992) 508.
- [89] A. Barkan, N. D'Angelo, and R. L. Merlino, Experiments on ion-acoustic waves in dusty plasmas, *Planetary and Space Science*, **44** (1996) 239-242.
- [90] Y. Nakamura, H. Bailung and P. K. Shukla, Observation of ion-acoustic shocks in a dusty plasma, *Physical review letters*, **83** (1999) 1602.
- [91] D. Angelis, V. Formisano, and M. Giordano, Ion plasma waves in dusty plasmas Halley's comet, *Journal of plasma physics*, **40** (1988) 399-406.
- [92] N. D'Angelo, Ion-acoustic waves in dusty plasmas, *Planetary and Space Science*, **42** (1994) 507-511.
- [93] D. B. Melrose, *Instabilities in space and laboratory plasmas*, Cambridge University Press, 1986.
- [94] Lord Rayleigh, *Proc. London Math Soc*, **14** (1883) 170.
- [95] Goldston, J. Robert and Paul Harding Rutherford, *Introduction to plasma physics*, CRC Press 1995.

- [96] <http://wordpress.mrreid.org/wp-content/uploads/2012/10/rayleigh-taylor.jpg>.
- [97] L. Kelvin, *Philosophical Magazine*, **42** (1871) 362–377 .
- [98] S. Chandrasekhar, *Hydrodynamic and Hydromagnetic Stability*, Oxford UK 1961.
- [99] Ofman, Leon, and B. J. Thompson, SDO/AIA observation of Kelvin–Helmholtz instability in the solar corona, *The Astrophysical Journal Letters*, **734** (2011).
- [100] N. D'Angelo, Ultralow frequency fluctuations at the polar cusp boundaries, *Journal of Geophysical Research*, **78** (1973) 1206–1209.
- [101] SckopkeN, et al, Structure of the low-latitude boundary layer, *J. Geophys. Res.*, **86** (1981) 2099.
- [102] N. d'Angelo, Low-frequency electrostatic waves in dusty plasmas, *Planetary and Space Science*, **38** (1990) 1143–1146.
- [103] Rawat, S. P. S., and N. N. Rao, Kelvin-Helmholtz instability driven by sheared dust flow *Planetary and space science*, **41** (1993) 137–140.
- [104] Garde, V. Seema , et al. Prostate secretory protein (PSP94) suppresses the growth of androgen-independent prostate cancer cell line (PC3) and xenografts by inducing apoptosis, *The Prostate*, **38** (1999) 118–125.
- [105] F. Verheest, *Waves in dusty space plasmas*, Vol. **245**, Springer Science & Business Media, 2001.
- [106] Banerjee, D., M. S. Janaki, and N. Chakrabarti, Shear flow instability in a strongly coupled dusty plasma, *Physical Review E*, **85** (2012) 066408.
- [107] Li, Lu, Li Zhong-Yuan, and Liu Zhen-Xing, Effect of dust charge fluctuations on Kelvin–Helmholtz instability in a cold dust plasma, *Physics of Plasmas*, **7** (2000) 424–427.
- [108] Ishihara, Osamu, Complex plasma dusts in plasma, *Journal of Physics D Applied Physics*, **40** (2007).

- [109] H. Zhao, G. S. P. Castle, I. I. Linculet and A. G. Bailey, *IEEE Trans. Ind. Appl.*, **39** (2003) 612.
- [110] Zheng-Xiong Wang, Yue Liu, Jin-Yuan Liu and Xiaogang Wang, *Phys. Plasmas*, **12** (2005) 014505.
- [111] C. K. Goertz, *Rev. Geophys*, **27** (1989) 271.
- [112] R.L. Merlino, and Goree, *J. Phys. Today*, **57** (2004) 32.
- [113] F. Verheest, *Waves in Dusty Plasmas*, Dordrecht Kluwer Academic Publishers, 2000.
- [114] Li, F., O. Havnes, and F. Melandsø Longitudinal waves in a dusty plasma, *Planetary and Space Science*, **42** (1994) 401-407.
- [115] P. K. Shukla, Low-frequency modes in dusty plasmas, *Physica Scripta*, **45** (1992) 504.
- [116] Havnes, O., A streaming instability interaction between the solar wind and cometary dust, *Astronomy and Astrophysics*, **193** (1988) 309-312.
- [117] Hartquist, T. W., O. Havnes, and G. E. Morfill, The effects of dust on the dynamics of astronomical and space plasmas, *Fundamentals of Cosmic Physics*, **15** (1992) 107-142.
- [118] Bharuthram, R., H. Saleem, and P. K. Shukla, Two-stream instabilities in unmagnetized dusty plasmas, *Physica Scripta*, **45** (1992) 512.
- [119] N. d'Angelo, The Rayleigh-Taylor Instability in Dusty Plasmas, *Planetary Space Sci.*, **41** (1993) 469-474.
- [120] Jana, M. R., A. Sen, and P. K. Kaw, Influence of grain charge fluctuation dynamics on collective modes in a magnetized dusty plasma, *Physica Scripta*, **51**(1995) 385.
- [121] Varma, R. K., and P. K. Shukla, Linear and nonlinear Rayleigh-Taylor modes in nonuniform dusty magnetoplasmas, *Physica Scripta*, **51** (1995) 522.

- [122] N. d'Angelo, and Bin Song, The Kelvin-Helmholtz instability in dusty plasmas, *Planetary and Space Science*, **38** (1990) 1577-1579.
- [123] Luo, Q. Z., N. D'Angelo, and R. L. Merlino, The Kelvin-Helmholtz instability in a plasma with negatively charged dust, *Physics of Plasmas*, **8**(2001) 31-35.
- [124] Rawat, S. P. S., and N. N. Rao, Kelvin-Helmholtz instability driven by sheared dust flow, *Planetary and space science*, **41** (1993) 137-140.
- [125] Willig, J., R. L. Merlino, and N. D'Angelo, Experimental study of the parallel velocity shear instability, *Physics Letters A*, **236** (1997) 223-226.
- [126] Zaheer, S., and G. Murtaza, Weibel instability with non-Maxwellian distribution functions, *Physics of plasmas*, **14** (2007) 022108.
- [127] Qureshi, M. N. S., et al. Solar wind particle distribution function fitted via the generalized kappa distribution function Cluster observations, *AIP Conference Proceedings*, **679** AIP, (2003).
- [128] Chuang, S-H., and L-N. Hau, The characteristics of ion acoustic solitons in non-Maxwellian plasmas, *Physics of Plasmas*, **16** (2009) 022901.
- [129] Zaheer, S., G. Murtaza, and H. A. Shah, Some electrostatic modes based on non-Maxwellian distribution functions, *Physics of Plasmas*, **11** (2004) 2246-2255.
- [130] Lee, Myoung-Jae, Landau damping of dust acoustic waves in a Lorentzian plasma, *Physics of plasmas*, **14** (2007) 032112.
- [131] D'Angelo, Nicola, Kelvin-helmholtz instability in a fully ionized plasma in a magnetic field, *The Physics of Fluids*, **8** (1965) 1748-1750.
- [132] V. Pierrard, M. Lazar, Kappa distributions: theory and applications in space plasmas, *Solar Physics*, **267** (2010) 153-174.
- [133] Yaroshenko, V. V., F. Verheest, and G. E. Morfill, Dnst-acoustic waves in collisional dusty plasmas of planetary rings, *Astronomy & Astrophysics*, **461** (2007) 385-391.